Two distinct oscillatory auxin signals define the plasticity of lateral rooting in *Arabidopsis thaliana*

Chengzhi Ren[1,2], Jule Bodendorf[1,2], Miguel A. Moreno-Risueno[3], Jürgen Kleine-Vehn[1,2]*

[1]Institute of Biology II, Molecular Plant Physiology (MoPP), University of Freiburg; Freiburg, 79104, Germany.

[2]Center for Integrative Biological Signalling Studies (CIBSS), University of Freiburg; Freiburg, 79104, Germany.

[3] Centro de Biotecnología y Genómica de Plantas (Universidad Politécnica de Madrid (UPM), Instituto Nacional de Investigación y Tecnología Agraria y Alimentaria-CSIC (INIA-CSIC)); Madrid, 28223, Spain.

Abstract

The phytohormone auxin defines lateral root pre-branch sites (PBS) in the growing primary root tip. How PBS contribute to the plasticity of the root system architecture remains incompletely understood[1,2,3,4]. Here, we reveal in the model plant *Arabidopsis thaliana* that two distinct oscillatory systems for the phytohormone auxin coordinate the spatial and temporal identity of PBS, jointly defining the lateral root density. We followed auxin signalling dynamics for days and thereby detected a systemic auxin signal oscillating along the mature primary root, where PBS potentially form functional root branches. While a previously proposed local oscillatory auxin zone spatially primes the PBS in the growing root

tip, we reveal that the systemic oscillatory auxin signal temporally controls the auxin-dependent identity of these PBS. Light perception in the shoot defines the strength of the systemic auxin signal and thereby controls the auxin-reliant ability of PBS to develop into lateral roots. Moreover, PHYB and CRY1 mediate the light-dependent integration of other environmental signals, such as ambient temperature, into the control systemic auxin signalling and lateral root density. Our work reveals how two spatially distinct oscillatory auxin signals define the plasticity of plant root development in response to fluctuating conditions.

Main

De novo organogenesis is a hallmark of the remarkable plasticity and adaptability in plants. In the context of root system architecture, lateral root (LR) formation is a critical process that enhances nutrient and water uptake, providing stability and resilience. Although several models have been proposed, the mechanism of lateral root initiation, especially during the early stage, remains an active area of research. A hypothesis suggests that the sites of presumptive LR development are predetermined along the primary root axis through a mechanism which involves the so-called "root clock"[1,2,3,4]. According to this, a localized oscillatory signal of the phytohormone auxin in the elongation zone of the main root (oscillatory zone) primes cells to become the LR pre-branch sites (PBS)[2]. Although the root clock model can describe the regular formation of PBS, there remain open questions regarding an apparent lack of plasticity in this system and the extent to which PBS are predetermined to ultimately develop into LR[5].

43 We used prolonged imaging of the synthetic, auxin-responsive *DR5* promoter fused to
44 a luciferase reporter (*pDR5::Luc*)[2] to visualize the nuclear auxin output signalling and
45 therewith PBS dynamics for days at constant light (120 $\mu mol \cdot m^{-2} \cdot s^{-1}$) and temperature
46 (21°C) conditions. Therewith, we revealed that a substantial fraction of the PBS lost the
47 auxin signal in time and did not give rise to LR development (Supplementary Fig. 1).
48 We, hence, addressed the currently elusive mechanism that decisively defines the
49 transient or persistent nature of the auxin-reliant PBS and its contribution to control LR
50 density.

51 **Light quantitatively controls a systemic oscillatory auxin signal**

52 To analyze the long-term dynamics of *DR5* luciferase activity, we utilize kymograph
53 representations, which are graphical depictions of spatial position (top to bottom) over
54 time (left to right), essentially capturing the dynamic changes along a root in a single
55 image. This approach allowed us to detect a repeated fluctuation of auxin signalling
56 over time. These dynamics were present along the primary root, including the PBS,
57 suggesting a systemic synchronization (Fig. 1a,b and Supplementary Fig. 2a;
58 Supplementary Fig. 3). In our constant growth condition, the frequency of this systemic
59 auxin signalling fluctuation followed a normal distribution with a period of around 24
60 hours (Fig. 1c, Supplementary Fig. 2b). We accordingly define these dynamics
61 hereafter as a systemic oscillatory auxin signal. We subsequently assessed if
62 environmental factors, such as light intensity, affect this systemic oscillatory auxin
63 signal. When compared to control 120 $\mu mol \cdot m^{-2} \cdot s^{-1}$ light conditions (hereafter referred

64 to as comparatively high light, HL), a reduction of the light intensity to 50 μmol·m^{-2}·s^{-1} (hereafter referred to as comparatively medium light, ML) did not affect the frequency of the systemic auxin oscillations (Fig. 1d,e and Supplementary Fig. 2c,d) but did quantitatively decrease the overall intensity of the systemic auxin signal (Fig. 1f). Notably, the systemic auxin signalling was undetectable at a light intensity of 20 μmol·m^{-2}·s^{-1} (hereafter referred to as comparatively low light, LL) (Fig. 1g and Supplementary Fig. 4).

71 Based on these results, we propose that light quantitatively controls a systemic oscillatory auxin signal. Next, we addressed whether the systemic auxin signalling dynamics contribute to the transient nature of auxin-reliant PBS. Notably, despite the varying strength of systemic auxin signalling at different light intensities, we observed similar quantities of established PBS under HL, ML, and LL conditions (Fig. 1h), indicating that the initial priming of PBS is largely independent of light intensity. However, we observed a correlation between the impediment of systemic auxin signalling and a steep increase in transient auxin signal in PBS at LL conditions (Fig. 1i). This result suggests that light intensity contributes to maintaining the auxin-reliant identity of PBS, correlating with a quantitative impact on systemic auxin oscillation.

81 **Light-reliant systemic auxin signal oscillations define PBS identity**

82 To specifically address the light dependency of already formed PBS, we monitored PBS formation in 5-day-old *pDR5::Luc* seedlings under HL conditions for 48 hours and afterwards exposed them either to LL conditions or maintained them under HL as a

control. After transferring seedlings from HL-to-LL conditions, the systemic auxin signalling completely ceased, observing the last oscillatory peak after 8 hours (Fig. 2a and Supplementary Fig. 5a). Additionally, although the total quantity of PBS was similar under both light conditions (Supplementary Fig. 6), the HL-to-LL transfer revealed that light intensity is critical to maintaining auxin signalling in PBS when compared to seedlings kept in HL (Fig. 2c,d). These findings confirm that light intensity is crucial to maintaining the systemic oscillatory auxin signal and PBS identity.

Contrariwise, we also monitored PBS formation in 5-day-old *pDR5::Luc* seedlings under LL conditions for 48 hours and subsequently transferred the seedlings either to HL conditions or kept them at LL as a control. In this condition, systemic auxin dynamics recovered around 18 hours after transferring from LL-to-HL (Fig. 2b and Supplementary Fig. 5b). Moreover, HL increased the recovery of auxin signalling in PBS when compared to those kept in LL (Fig. 2c,d). This finding again pinpoints the positive impact of light on systemic auxin signalling and its ability to reactivate auxin-reliant PBS.

Next, we tested if the light-dependent modulation of auxin in PBS indeed contributes to the reshaping of the root system architecture. To ensure the light effects are independent of LR priming, we transferred 7-day-old seedlings between different light conditions and analyzed three days later the LR appearance in a defined section of the main root (grown between days 4 and 7; see marks in Figure 2e). We observed a strong decrease in LR density when transferring roots from HL-to-LL compared to those

106 maintained at HL (Fig. 2e,f). Conversely, LR density significantly increased when
107 transferring from LL-to-HL as compared to those kept at LL (Fig. 2e,f). This set of data
108 confirms that light conditions control auxin-dependent PBS and thereby LR density.
109 Accordingly, we propose that light quantitatively controls systemic oscillatory auxin
110 signals, thereby temporally defining the identity of previously primed PBS and
111 ultimately LR spacing.

112 **Systemic auxin signal controls PBS identity at high ambient temperature**

113 We hypothesize that while the auxin oscillation zone enables the regular priming of
114 PBS during main root growth, a systemic oscillatory auxin signal could integrate
115 various environmental information into lateral root spacing. To further test this
116 assumption, we introduced variation in ambient temperature. Temperature and light
117 signalling both play a crucial role in shaping root system architecture and are in part,
118 molecularly interconnected[6]. Nonetheless, the existing literature reveals inconsistent
119 findings, suggesting that elevated ambient temperatures can exert both positive and
120 negative effects on lateral rooting within and across different species[7,8,9,10,11,12,13]. To
121 shed light on this seemingly complex role, we initially tested whether temperature also
122 affects auxin signalling dynamics in the root, we transferred 5-day-old *pDR5::Luc*
123 seedlings from a control temperature of 21°C to a high ambient temperature (HT) of
124 29°C at constant HL condition. By monitoring the root luminescence after the transfer,
125 we observed an overall increase of auxin signalling in the oscillation zone
126 corresponding with an increased signal in the kymograph diagonal (Fig. 3a,b), which

127 also correlated with an increased number of PBS (Fig. 3a,c). However, the vast majority
128 of auxin-reliant PBS appeared transiently, aligning with a severe systemic disruption of
129 auxin signalling over time (Fig. 3d,e, Supplementary Fig. 7).

130 Our results, hence, suggest that HT initially imposes a positive effect on initiating PBS
131 but subsequently limits the systemic auxin signal along the primary root. Contrary to
132 this observation, the lateral root primordia (LRP) (Supplementary Fig. 8) and overall
133 LR density (Fig. 3f,g) were not inhibited by HT but showed even slight enhancement
134 when compared to the control. To address this apparent contradiction, we initially
135 assessed if the systemic reduction of *pDR5::Luc* at higher temperatures could relate to
136 reduced enzymatic activity of luciferase at higher temperature. The reported midpoint
137 of the unfolding transition temperature of the luciferase enzyme *in vitro* is around 34°C,
138 which is further stabilized by osmolytes[14]. In agreement, luciferase activity in
139 *p35S::Luc* expression control lines did not decrease when transferred to 29 °C
140 (Supplementary Fig. 9). Notably, *p35S::Luc* showed at both temperatures an
141 enhancement over time, and the signal was consistently higher at 29 °C, which may
142 relate to variable 35S promoter activity in response to environmental changes or
143 developmental cues[15]. We conclude that the systemic decrease in *pDR5::Luc* dynamics
144 at high temperatures is not due to changes in enzymatic luciferase activity.

145 To further address the paradox of auxin dynamics and root system architecture, we
146 extended our imaging of the auxin output signalling to 8 days. Thereby, we observed a
147 recovery of the systemic auxin signalling around 70 hours after transferring seedlings

148 to HT conditions (Fig. 3h and Supplementary Fig. 10). The systemic peak in auxin
149 correlates with the reactivation of PBS, ultimately resulting in an increase in persistent
150 PBS at HT (Fig. 3h,i). Notably, the number of recovered, persistent PBS under this
151 condition is remarkably similar to the number in the control temperature condition (Fig.
152 3i). The reactivation of PBS strictly occurs simultaneously or after recovery of systemic
153 auxin peak (Fig. 3h, Supplementary Fig. 10), suggesting again that a systemic auxin
154 signal enables the integration of environmental cues into the temporal control of already
155 primed PBS.

156 **Light perception modulates high temperature-dependent control of auxin-reliant**
157 **PBS identity**

158 To further address that the systemic auxin signal indeed integrates environment
159 information into lateral rooting, we quantitatively lowered the HT-induced recovery of
160 the systemic auxin signal, using medium light conditions. Accordingly, we grew
161 *pDR5::Luc* seedlings at 21°C and HL and transferred 5-day-old seedlings to HT and
162 ML conditions. Similar to seedlings at HL (Fig. 3), HT also increased the auxin
163 signalling output at the local oscillation zone (Fig. 4a,b), correlating with initially
164 enhanced PBS priming at ML conditions when compared to the control (Fig. 4c).
165 Comparable to the HL condition, the formed PBS showed transient auxin signals, being
166 reflected by a strong, systemic disruption of auxin signalling in the mature root.

167 The HT also induced a temporal decline (Fig. 4d,e and Supplementary Fig. 11) and
168 systemic recovery of auxin signalling in ML conditions (Fig. 4f,g and

169 Supplementary Fig. 12). Importantly, the recovery of the systemic signal was, as
170 anticipated, quantitatively reduced (Fig. 4h) when compared to HL conditions. Notably,
171 the systemic auxin recovery was also temporarily delayed, occurring around 100 hours
172 after the transfer (Fig. 4f,g and Supplementary Fig. 12). In agreement with our
173 assumptions, ML-dependent reduction in systemic auxin signal also reduced the
174 recovery of auxin-reliant PBS (Fig. 4i) when compared to HL conditions. This set of
175 data strongly supports that light-dependent, systemic auxin signalling defines the
176 transient or persistent nature of PBS. Moreover, our data suggests that light quantity
177 modulates the negative impact of HT on PBS progression.

178 We next tested whether the proposed light-dependent modulation of ambient
179 temperature response indeed defines root system architecture. In contrast to the limited
180 effect of HT on LR density under HL conditions (Fig. 3), HT induced a strong reduction
181 in the density under ML conditions (Fig. 4j,k), confirming that light quantity indeed
182 contextualizes the integration of ambient temperature into root system architecture.

183 Next, we tested if this contextualizing mechanism defines not only PBS identity but
184 also blocks the LRP development. Whereas the LR density was decreased in these
185 conditions, we observed a quantitively similar amount of LRP when compared to the
186 control condition (Supplementary Fig. 13). This finding suggests that light-modulated
187 HT response does not primarily block LRP progression but impacts on PBS identity. In
188 agreement with its impediment in systemic auxin signalling, we observed that the HT-
189 dependent inhibition of lateral rooting was further enhanced under LL conditions

190 (Supplementary Fig. 14). This set of data suggests that systemic oscillation of auxin
191 integrates environmental signals, such as light and temperature, into the temporal
192 control of PBS, contributing significantly to the root system architecture. We hence
193 propose that the effect of high ambient temperature on lateral rooting is conditional,
194 which can explain the seemingly disparate literature on high temperature and its impact
195 on lateral rooting[7,8,9,10,11,12,13].

196 Besides its impact on lateral rooting, high temperature also enhances main root growth
197 in an auxin-dependent manner[16,17,18]. Moreover, it has been proposed that the priming
198 of lateral roots may depend on the interplay of auxin and main root growth
199 dynamics[19,20]. Hence, HT could indirectly affect lateral rooting by impacting primary
200 root growth. Therefore, we next address whether HT-induced main root growth is linked
201 to lateral rooting under our conditions. HT induced main root growth in HL, but this
202 effect was abolished in ML conditions, which is conversely to its impact on lateral
203 rooting (Supplementary Fig. 15a,b). These findings indicate that HT affects lateral
204 rooting and main root growth via distinct mechanisms.

205 **Oscillatory IAA14 coordinates systemic auxin signalling to modulate lateral root**
206 **PBS**

207 To further address the here proposed contextualizing role of auxin in light- and HT-
208 dependent inhibition of lateral rooting, we transferred 4-day-old seedlings to 29°C or
209 21°C under ML conditions for 3 days and subsequently sprayed either with the
210 endogenous auxin indole-3-acetic acid (IAA; 0.2 μM), auxin antagonist auxinole (20

211 μM), or Dimethyl sulfoxide (DMSO) as a solvent control. We analyzed lateral root
212 density in these root sections after an additional 7 days of HT treatment. The application
213 of auxin completely suppressed the HT-dependent inhibition of lateral rooting at ML
214 condition (Fig. 5a-c). In contrast, auxinole-dependent inhibition of auxin signalling led
215 to enhanced HT-induced inhibition of lateral root density compared to DMSO (Fig. 5a-
216 c). These results confirm that HT-dependent inhibition of lateral rooting is linked to
217 auxin responses.
218 We subsequently focused on SOLITARY ROOT/Indole-3-Acetic Acid inducible 14
219 (SLR/IAA14), a key repressor of nuclear auxin responses being involved in limiting
220 lateral root initiation. The prominent gain-of-function *solitary root* (*slr-1*) mutant
221 carries stabilized, auxin-insensitive *IAA14*, causing constitutive auxin repression and
222 complete loss of lateral roots, which might be independent of PBS priming[21,22,23].
223 To investigate the real-time transcription of *IAA14* in the root, we fused the promoter
224 of *IAA14* to a luciferase reporter (*pIAA14::Luc*). By monitoring the luminescence in the
225 root, we observed a continuous, non-oscillatory transcription of *IAA14* in the auxin
226 oscillation zone of the root tip (Supplementary Fig. 16). This aligns with the hypothesis
227 that *IAA14* operates independently of PBS priming, although an indirect effect cannot
228 be disregarded. On the contrary, we observed systemic oscillatory dynamics of the
229 *IAA14* reporter along the primary root and PBS, which is reminiscent of the synthetic
230 auxin reporter *pDR5::Luc* dynamics under control conditions (Fig. 5d,e, Supplementary
231 Fig. 17a). Additionally, The frequency of *IAA14* reporter fluctuation also followed a
232 normal distribution with a period of around 24 hours (Supplementary Fig. 17a-c),

233 similar to the oscillatory frequency of *pDR5::Luc* (Fig. 1c,e, Supplementary Fig. 2).
234 Notably, *IAA14* reporter signal gradually became undetectable in primary root and PBS
235 under LL condition (Supplementary Fig. 18), consistent with the disappearance of the
236 *pDR5::Luc* signals (Fig. 1, Supplementary Fig. 4). These observations reaffirmed that
237 light quantitatively modulates the systemic oscillatory auxin signalling. Similar to the
238 synthetic *DR5* auxin signalling reporter, *IAA14* expression systemically decreased in
239 both the primary root and PBS after transferring to HT under ML conditions (Fig. 5f,g).
240 Unlike the strong systemic recovery of *pDR5::Luc* under HT (Fig. 3h, Fig. 4f,
241 Supplementary Fig. 10 and Supplementary Fig. 12), *pIAA14::Luc* expression recovered
242 specifically in the PBS (Fig. 5f,g). After transferring to HT and HL conditions, *IAA14*
243 expression decreased exclusively in the primary root but remained persistent in
244 individual PBS (Supplementary Fig. 19). This set of data suggests that temperature and
245 light-dependent control of systemic auxin signalling defines IAA14-reliant lateral
246 rooting.
247 Next, we genetically interfered with these auxin signalling dynamics by introducing the
248 *slr-1* mutation into the *pDR5::Luc* background by genetic crossing. We detected a
249 systemic oscillatory auxin signal along the primary root of the *slr-1* mutant (Fig. 5h,i).
250 This suggests that SLR is not required to generate the systemic auxin signal, but
251 functions a downstream effector regulating PBS capacity to develop LRs. In agreement
252 with this assumption, the PBS failed to be temporarily maintained in *slr-1* between the
253 systemic oscillation peaks of auxin (Fig. 5h,i). This set of data reinforces that the
254 integration of systemic auxin signalling is critical for persistent PBS identity and its

ability to develop into lateral roots.

PHYB and CRY1 mediate shoot-perceived light modulating effect of high ambient temperature on lateral rooting

Our collective findings highlight the principal role of light in modulating temperature-dependent systemic auxin signalling and subsequent lateral rooting. We subsequently assessed where light is perceived to contextualize the temperature-sensitive lateral rooting. Therefore, we used light exposure of the root or shoot only to dissect where the light signal that modulates lateral rooting is perceived. We found that light exposure of the shoot is not only essential for lateral root development but also sufficient to modulate the temperature-dependent lateral rooting (Supplementary Fig. 20a-c). Hence, we assume that light perception in the shoot contributes to the auxin-reliant lateral rooting mechanism. Photosynthetic sucrose is an important determinant of lateral rooting[24]. However, the presence or absence of sucrose in the media did not affect the pattern of lateral rooting by HT under both HL and ML conditions (Supplementary Fig. 20d-f). This finding implies that photosynthetic sucrose is not the contextualizing signal in this context, pinpointing a light perception mechanism. Subsequently, we investigated the light perception mechanism of the light-modulated HT-dependent repression of lateral rooting. Mutations in the *phytochrome B* (*phyB*) red and far-red light photoreceptor caused hypersensitivity to HT-induced repression of lateral rooting at ML conditions when quantitatively compared to the wild-type (Supplementary Fig. 21a-c). In addition to functioning as a light sensor, PHYB also acts as a thermosensor[25].

276 However, the increased hypersensitivity to HT-induced repression of lateral rooting
277 observed in the *phyB-9* mutant suggests that PHYB does not function as the
278 thermosensor in this process (Supplementary Fig. 21a-c). Moreover, we detected a
279 similar hypersensitivity to HT at ML condition in mutants of the blue light receptor
280 *cryptochrome 1* (*CRY1*) (Supplementary Fig. 21a-c). Notably, triple mutants of
281 *phyBcry1cry2* not only enhanced hypersensitivity to HT-induced repression of lateral
282 rooting at ML conditions compared to single mutants of *phyB-9* and *cry1-304*
283 (Supplementary Fig. 21a-c), but also caused sensitivity to HT at HL conditions when
284 compared to the wild-type, which was not observed in the single mutant of *phyB-9* and
285 *cry1-304* (Fig. 5j-l). In contrast, the genetic interference with *phytochrome A* (*phyA*) or
286 *phototropins* (*PHOTs*) had no major impact on the high-temperature-induced repression
287 of lateral root development (Supplementary Fig. 22a-e). We accordingly conclude that
288 *PHYB* and *CRY1* jointly mediate the light-modulated integration of ambient
289 temperature into the root system architecture.

290 *PHYB* and *CRY1* both mediate light signals by regulating *PHYTOCHROME*
291 *INTERACTING FACTORS* (*PIFs*) and *ELONGATED HYPOCOTYL5* (*HY5*) module,
292 which is also known to integrate light quality during the shade avoidance response into
293 the rate of lateral rooting[26,27,28]. However, neither the quadruple mutant *pif1,3,4,5* (*pifQ*),
294 nor *hy5-215* mutant was distinguishable from the wild type in regards to HT-dependent
295 lateral rooting under ML condition (Supplementary Fig. 22a and f-i). This suggests a
296 molecularly distinct mechanism for the integration of light quality during shade
297 avoidance and the light quantity-dependent modulation of HT into lateral rooting.

Concluding remarks

Mechanistically, we propose that the PHYB- and CRY1-mediated light quantity in the shoot defines the strength of a systemic oscillatory auxin signal in the main root, thereby defining the auxin-dependent identity of lateral root PBS. The light-dependent, systemic auxin dynamics also modulate HT-dependent control of PBS progression to lateral roots, suggesting a general mechanism for environmental signal integration. However, the mechanism by which shoot-sensed light signalling modulates systemic oscillatory auxin signals in the root remains to be addressed. Light receptors are well known for shaping plant architecture by modulating key components of the circadian clock[29]. Notably, the 24-hour rhythm of systemic auxin oscillations may pinpoint a potential role for the circadian clock in signal transmission. While this aspect requires further investigation, it is noteworthy that the circadian clock regulates at least some auxin-mediated transcriptional responses[30]. Conceptually, our work illustrates that two oscillatory systems define LR spacing. While a local auxin oscillation zone regulates the regular priming of PBS during main root growth, the systemic oscillatory auxin signal along the main root integrates environmental information, such as light and temperature, to control the PBS identity in time and eventually its progression to become lateral roots. This framework reveals how plants mechanistically use distinct oscillatory signals of the same regulator to combine robustness and plasticity into *de novo* organogenesis.

References

1. De Smet I., et al., Auxin-dependent regulation of lateral root positioning in the basal meristem of Arabidopsis. *Development* **134**, 681–690 (2007).

2. Moreno-Risueno AM., et al., Oscillating Gene Expression Determines Competence for Periodic Arabidopsis Root Branching. *Science* **329**, 1306–1311 (2010).

3. Xuan W., De Gernier H., Beeckman T., The dynamic nature and regulation of the root clock. *Development* **147**, dev181446 (2020).

4. Perianez-Rodriguez J., et al., An auxin-regulable oscillatory circuit drives the root clock in Arabidopsis. *Sci. Adv.* **7**, eabd4722 (2021).

5. Kircher S., Schopfer P., The plant hormone auxin beats the time for oscillating light-regulated lateral root induction. *Development* **145**, dev169839 (2018).

6. Qi L., et al., Integration of light and temperature signaling pathways in plants. *J. Integr. Plant Biol.* **64**, 393–411 (2022).

7. González-García M. P., et al., Temperature changes in the root ecosystem affect plant functionality. *Plant Commun.* **4**, 100514 (2023).

8. Wang R., et al., HSP90 regulates temperature-dependent seedling growth in Arabidopsis by stabilizing the auxin co-receptor F-box protein TIR1. *Nat. Commun.* **7**, 10269 (2016).

9. Borniego M. B., Costigliolo-Rojas C., Casal J. J., Shoot thermosensors do not fulfil the same function in the root. *New Phytol.* **236**, 9–14 (2022).

10. Gray W. M., et al., High temperature promotes auxin-mediated hypocotyl elongation in Arabidopsis. *Proc. Natl. Acad. Sci. U. S. A.* **95**, 7197–7202 (1998).

11. Nagel K. A., Temperature responses of roots: impact on growth, root system architecture and implications for phenotyping. *Funct. Plant Biol.* **36**, 947–959 (2009).

12. Gladish D. K., Rost T. L., The effects of temperature on primary root growth dynamics and lateral root distribution in garden pea (Pisum sativum L., cv. “Alaska”). *Environ. Exp. Bot.* **33**, 243–258 (1993).

13. Vescio R., Abenavoli M. R., Sorgonà A., Single and Combined Abiotic Stress in Maize Root Morphology. *Plants (Basel)* **10**, 5 (2021).

14. Mehrabi M., Hosseinkhani S., Ghobadi S., Stabilization of firefly luciferase against thermal stress by osmolytes. *Int J Biol Macromol* **43**, 187-191 (2008).

15. Kiselev KV., et al., 35S promoter-driven transgenes are variably expressed in different organs of Arabidopsis thaliana and in response to abiotic stress. *Mol Biol Rep.* **48**, 2235-2241 (2021).

16. Feraru E., et al., PILS6 is a temperature-sensitive regulator of nuclear auxin input and organ growth in Arabidopsis thaliana. *Proc. Natl. Acad. Sci. U. S. A.* **116**, 3893–3898 (2019).

17. Gaillochet C., et al., HY5 and phytochrome activity modulate shoot-to-root coordination during thermomorphogenesis in Arabidopsis. *Development* **147**, dev192625 (2020).

18. Ai H., et al., Auxin-dependent regulation of cell division rates governs root thermomorphogenesis. *EMBO J.* **42**, e111926 (2023).

19. van den Berg T., et al., A reflux-and-growth mechanism explains oscillatory patterning of lateral root branching sites. *Dev. Cell* **56**, 2176-2191 (2021).

20. Reyes-Hernández B. J., Maizel A., Tunable recurrent priming of lateral roots in Arabidopsis: More than just a clock? *Curr. Opin. Plant Biol.* **76**, 102479 (2023).

21. Fukaki H., et al., Lateral root formation is blocked by a gain-of-function mutation in the Arabidopsis IAA14 gene. *Plant J.* **29**, 153–168 (2002).

22. Fukaki H., et al., Tissue-specific expression of stabilized SOLITARY-ROOT/IAA14 alters lateral root development in Arabidopsis. *Plant J.* **44**, 382–395 (2005).

23. De Smet I., et al., Auxin-dependent regulation of lateral root positioning in the basal meristem of Arabidopsis. *Development* **134**, 681-690 (2007).

24. Kircher S., Schopfer P., Photosynthetic sucrose drives the lateral root clock in Arabidopsis seedlings. *Curr. Biol*. **33**, 2201-2212 (2023).

25. Jung J. H., et al., Phytochromes function as thermosensors in Arabidopsis. *Science* **354**, 886–889 (2016).

26. Pierik R., Ballaré C. L., Control of Plant Growth and Defense by Photoreceptors: From Mechanisms to Opportunities in Agriculture. *Mol. Plant* **14**, 61–76 (2021).

27. van Gelderen K., et al., Far-Red Light Detection in the Shoot Regulates Lateral Root Development through the HY5 Transcription Factor. *Plant Cell* **30**, 101–116 (2018).

28. Zeng J., et al., Arabidopsis cryptochrome-1 restrains lateral roots growth by inhibiting auxin transport. *J. Plant Physiol.* **167**, 670–673 (2010).

29. Su C., et al., Coordinative regulation of plants growth and development by light and circadian clock. *aBIOTECH.* **2**, 176-189 (2021).

30. Covington MF., Harmer SL., The circadian clock regulates auxin signaling and responses in Arabidopsis. *PLoS Biol.* **5**, e227 (2007).

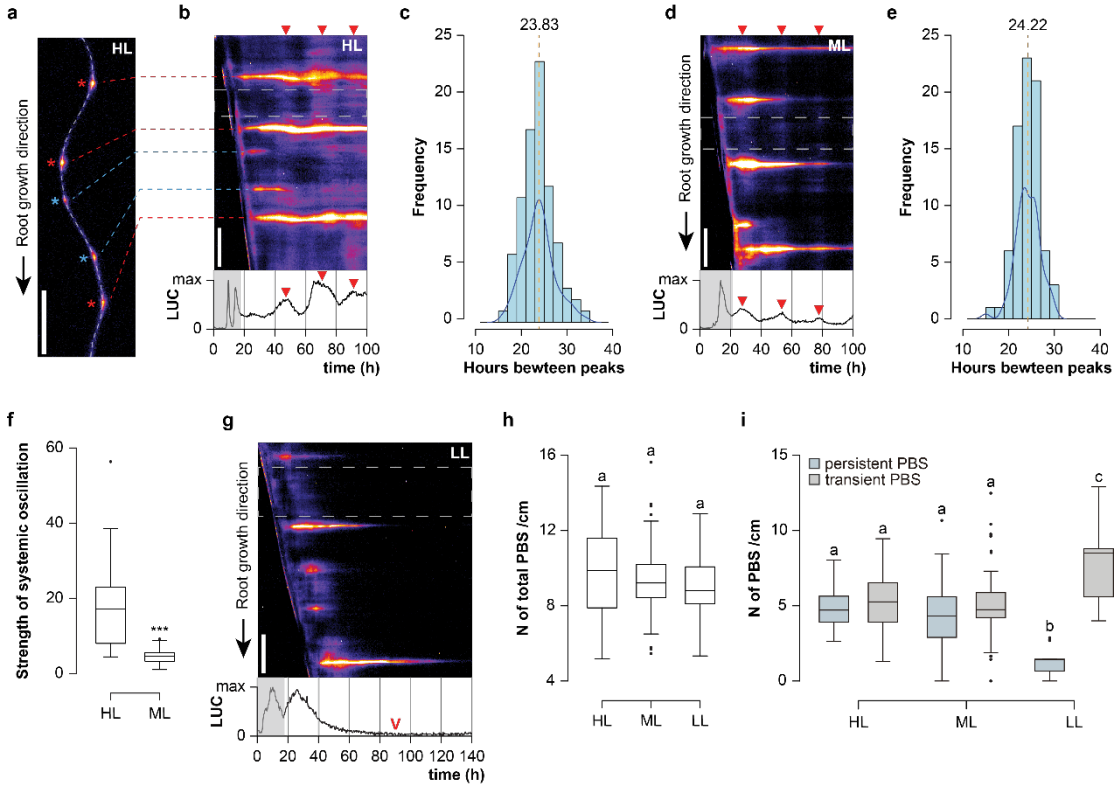

Figure 1. Light quantitatively defines a systemic auxin oscillation in main roots and pre-branch sites.

a-g, *pDR5::Luc* expressing root (**a**) was segmented (dashed line) for the respective kymograph (**b**). Asterisks and dashed lines mark the positions of persistent (red) and transient (blue) auxin signals in PBS. Kymographs display auxin signalling dynamics in high light (HL) (**b**), medium light (ML) (**d**) and low light (LL) (**g**) (Scale bar = 1 mm). Quantification of real-time luminescence is below the kymographs where the red triangles mark oscillatory peaks of systemic auxin signal (**b**, **d**). Red arrowhead denotes the downregulation of the systemic auxin signal (**g**). The dashed grey rectangle in the kymographs mark the region for the real-time plots (**b**, **d**, **g**). The shaded area in real-

time plots marked the signal originating from the root tip and root clock zone (**b**, **d**, **g**). Quantified distribution of the time intervals between oscillatory peaks of systemic auxin under (**c**) HL and (**e**) ML conditions (mean value marked by a yellow dashed line; n = 23 to 29; Anderson-Darling normality test, P-value = 0.4501 (**c**) and 0.177 (**e**)). (**f**) Quantified luminescence intensity of oscillatory peaks under HL and LL conditions (n = 20). **h**, Quantification of PBS density under HL, ML and LL conditions (n = 16 to 66). **i**, Quantification of persistent and transient auxin in PBS under HL, ML and LL conditions (n = 16 to 66). Paired and two-tailed student's t-test performed for (**f**) (P < 0.001***). Letters indicate values with statistically significant differences from one-way ANOVA performed for (**h**) (P > 0.05) and (**i**) (P < 0.0001).

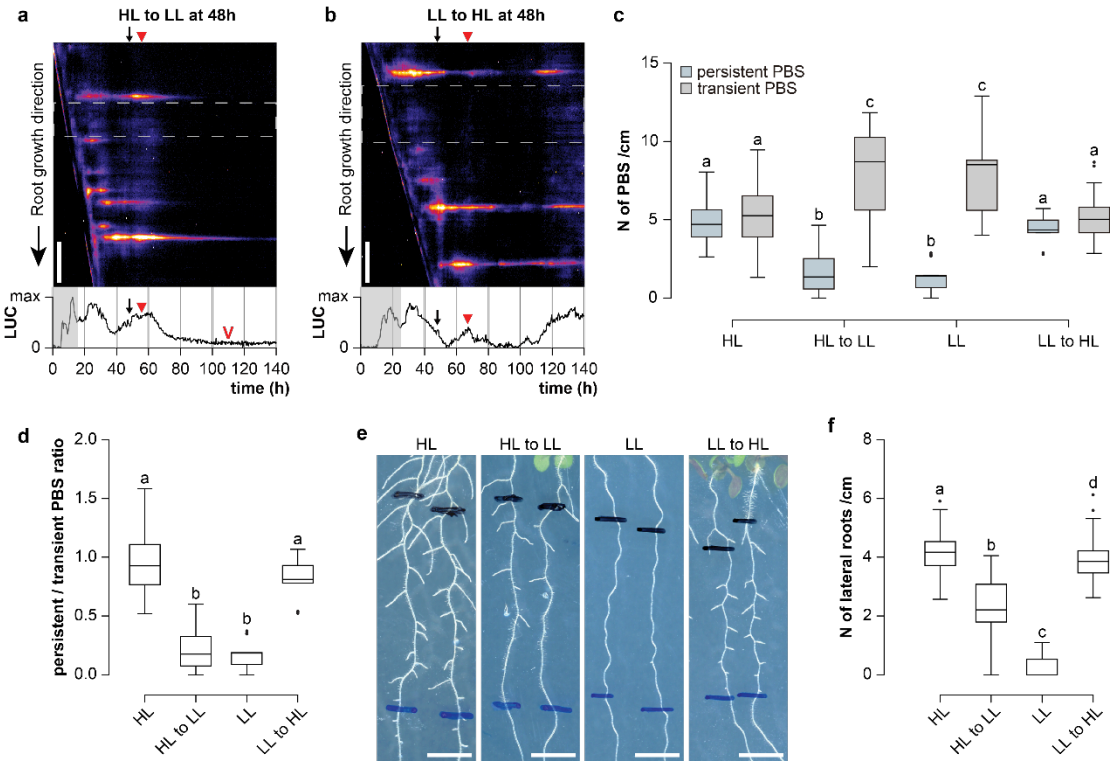

Figure 2. Light-reliant systemic auxin signal determines PBS dynamics and lateral rooting.

a-d, Kymograph and real-time quantification of relative luminescence show systemic auxin and PBS progression dynamics during light transitions from high light (HL) to low light (LL) (**a**) and LL-to-HL (**b**) (Scale bar = 1 mm). Black arrows mark the time of transfer (**a**, **b**). The red triangle marks the peak of the systemic auxin signal (**a**, **b**). The red arrowhead indicates that auxin signalling has reduced to the background level(**a**). The dashed grey rectangle marks the region for the real-time plots; The shaded area in real-time plots marked the signal originating from the root tip and root clock zone (**a**, **b**). Quantification (**c**) and the corresponding ratio (**d**) of persistent and transient auxin signal in PBS under both transitional and maintained light conditions (n = 16 to 38). **e**, **f**, Representative images of root systems (**e**) and quantification of LR density (**f**) under both maintained light conditions and transferred HL-to-LL and LL-to-HL (n = 58 to 61; Scale bar = 5 mm). Letters indicate values with statistically significant differences from one-way ANOVA performed for (**c**), (**d**) and (**f**) (P < 0.0001 for all).

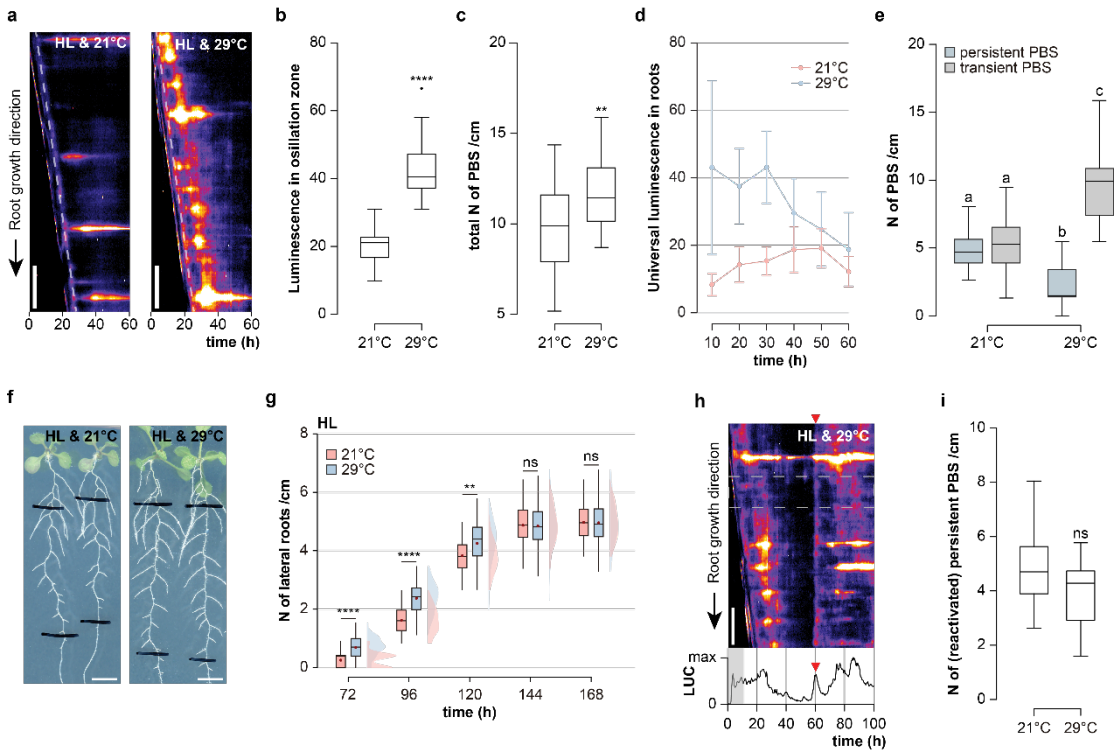

424 **Figure 3. High-temperature affects systemic auxin signal and PBS dynamics.**

425 **a**, Kymograph of *pDR5::Luc* expressing roots, showing the priming and progression of
426 PBS at 21°C and 29°C under high light (HL) conditions. The dashed line marks the
427 local oscillatory (root clock) zone (Scale bar = 1 mm). **b**, Quantification of average
428 luminescence in oscillatory zone over time in 21°C and 29°C under HL conditions (n =
429 24 to 30). **c**, Quantification of PBS density at 21°C and 29°C under HL conditions (n =
430 16 to 22). **d**, The quantified dynamic of *pDR5::Luc* signal in the main roots at 21°C and
431 29°C under HL conditions (Error bars represent standard deviation; n = 16 to 22). **e**,
432 Quantification of persistent and transient PBS at 21°C and 29°C under HL conditions
433 (n = 16 to 22). **f**, **g**, Representative images of the root system (**f**) and time series
434 quantification of LR density (**g**) at 21°C and 29°C under HL conditions (n = 54 to 55;
435 Scale bar = 5 mm). **h**, Long-term kymographs and real-time quantification of relative
436 luminescence showing the recovery of systemic auxin and PBS under 29°C and HL
437 condition. The red triangle marked the recovery peak of systemic auxin signal; The
438 dashed grey rectangle marks the region for the real-time plots; The shaded area in real-
439 time plots marked the signal originating from the root tip and root clock zone (Scale
440 bar = 1 mm). **i**, Quantified density of persistent PBS at 21°C and reactivated persistent
441 PBS at 29°C under HL condition during prolonged monitoring (n = 16 to 22). Paired
442 and two tailed student's t-test performed for (**b**), (**c**), (**g**) and (**i**) (P < 0.01** and <
443 0.0001****). Letters indicate values with statistically significant differences from one-
444 way ANOVA performed for (**e**) (P < 0.0001).

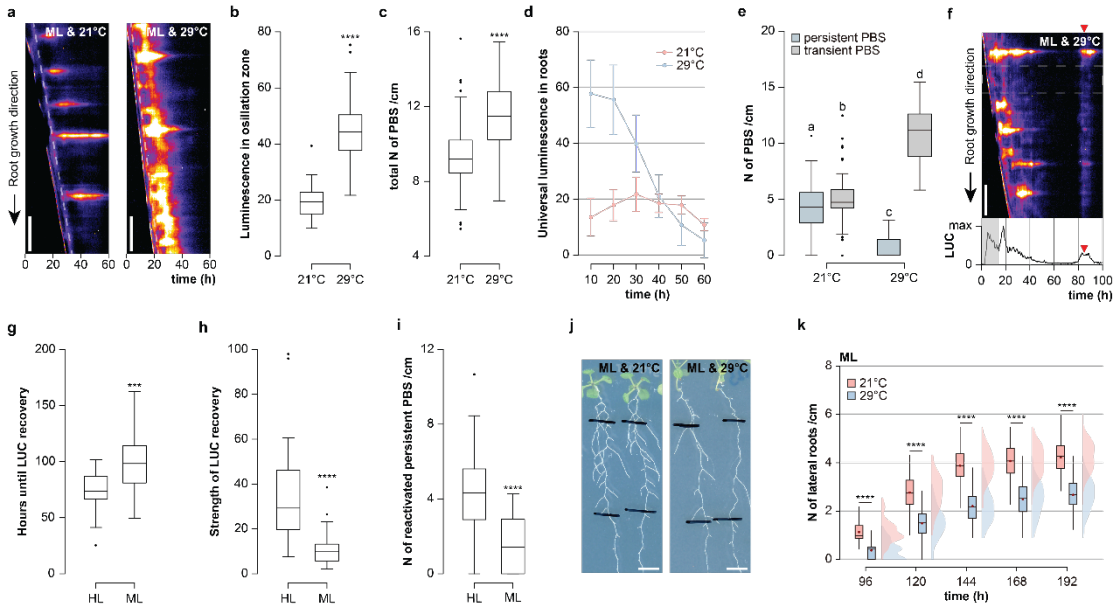

Figure 4. Light modulates high-temperature-dependent impact on systemic auxin signal and thereby lateral rooting.

a, Kymograph of *pDR5::Luc* expressing roots, showing the priming and progression of PBS at 21°C and 29°C under medium light (ML) conditions. The dashed line marks the local oscillatory (root clock) zone (Scale bar = 1 mm). **b**, Quantifying average luminescence in oscillatory zone over time at 21°C and 29°C under ML conditions (*n* = 24 to 40). **c**, Quantification of PBS density at 21°C and 29°C under ML conditions (*n* = 66). **d**, Quantified dynamic of universal *pDR5::Luc* in main roots at 21°C and 29°C under ML conditions (Error bars represent standard deviation; *n* = 16 to 32). **e**, Quantification of persistent and transient PBS at 21°C and 29°C under ML conditions (*n* = 66). **f**, Long-term kymographs and real-time quantification of relative luminescence showing the recovery of systemic auxin and PBS at 29°C under ML condition. The red triangle marks the recovery peak of the systemic auxin signal; The dashed grey rectangle marks the region for the real-time plots; The shaded area in real-

time plots marks the signal originating from the root tip and local oscillation (root clock) zone (Scale bar = 1 mm). **g**, **h**, Quantification of time until recovery (**g**) and strength (**h**) of systemic auxin signalling peak in primary roots after transferred at 29°C under ML and high light (HL) conditions (n = 24 to 48). **i**, Quantified density of reactivated persistent PBS at 29°C under ML and HL conditions (n = 24 to 48). **j-k**, Representative images of the root system (**j**) and time series quantification of LR density (**k**) at 21°C and 29°C under ML conditions (n = 54 to 55; Scale bar = 5 mm). Paired and two-tailed student's t-test performed for (**b**), (**c**), (**g**), (**h**), (**i**), (**k**) ($P < 0.001$*** and < 0.0001****). Letters indicate values with statistically significant differences from one-way ANOVA performed for (**e**) ($P < 0.0001$ for all).

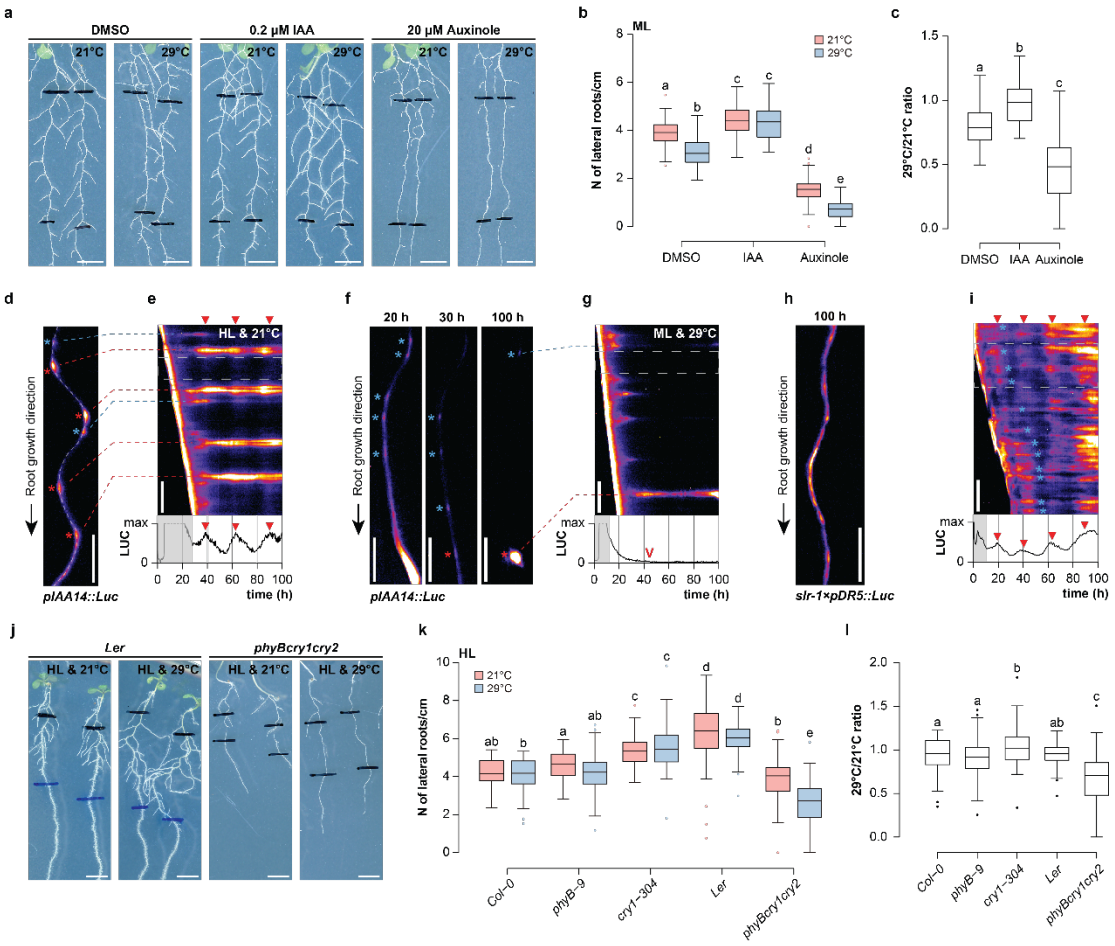

471 **Figure 5. Dynamic of *IAA14* integrate systemic auxin signalling into the identity**
472 **of PBS.**

473 **a**, **b**, Representative images of the root system (**a**) and quantification of LR density (**b**)
474 at 21°C and 29°C under DMSO, 0.2 μM IAA and 20 μM Auxinole spraying (n = 55
475 to 63; Scale bar = 5 mm). **c**, Calculated ratio of final LR density at 21°C and 29°C
476 spreading DMSO, 0.2 μM IAA and 20 μM Auxinole (n = 55 to 63). **d-g**, *pIAA14::Luc*
477 expressing root at 21°C under high light (HL) (**d**) and 29°C under medium light (ML)
478 (**f**). Asterisks and dashed lines (**d**, **f**) mark the positions of persistent (red) and transient
479 (blue) PBS. Kymographs display *pIAA14::Luc* dynamics at 21°C under HL (**e**) and
480 29°C under ML (**g**) (Scale bar = 1 mm). Quantification of real-time luminescence is
481 below the kymographs where the red triangles mark oscillatory peaks of *pIAA14::Luc*
482 signal (**e**, **g**). Red arrowhead denotes the downregulation of the *pIAA14::Luc* signal (**g**).
483 The dashed grey rectangle in the kymographs mark the region for the real-time plots (**e**,
484 **g**). The shaded area in real-time plots marks the signal originating from the root tip and
485 local oscillation (root clock) zone (**e**, **g**). **h**, **i**, *pDR5::Luc* expressing root (**h**) and
486 respective kymograph (**i**) in *slr-1* background (Scale bar = 1 mm). Blue asterisks mark
487 the positions of PBS-like pre-signals (**i**). Quantification of real-time luminescence is
488 below the kymographs where the red triangles mark oscillatory peaks of auxin signal
489 (**i**). The dashed grey rectangle in the kymographs mark the region for the real-time plots
490 (**i**). The shaded area in real-time plots marks the signal originating from the root tip and
491 local oscillation (root clock) zone (**i**). **j**, **k**, Representative images (**j**) and quantified LR
492 density (**k**) of *Col-0*, *Ler* wild types and light receptor mutants at 21°C and 29°C under

493 HL conditions (n = 45 to 72; Scale bar = 5 mm). **l**, Quantified ratio of LR density at
494 29°C to 21°C for *Col-0*, *Ler* wild types and light receptor mutants (n = 45 to 72). Letters
495 indicate values with statistically significant differences from one-way ANOVA
496 performed for (**b**), (**c**), (k) and (l) ($P < 0.0001$ for all).

497 **Materials and methods**

498 **Plant Materials**

499 The *Arabidopsis thaliana* ecotype *Columbia 0* (*Col-0*) and *Landsberg* (*Ler*) were used
500 as the wild type in this study. The *pDR5::Luc*[2] and *slr-1*[21] are in the ecotype *Col-0*
501 accession and was received from Stefan Kircher. The mutants of *phyA-211*[31], *phyB-9*[32],
502 *cry1-304*[33], *pif1,3,4,5*[34] and *hy5-215*[35] mutants are all in the *Col-0* accession and were
503 received from Andreas Hiltbrunner. The mutant of *phyBcry1cry2*[36] is in the ecotype Ler
504 accession and was received from Stefan Kircher. *pIAA14::Luc* and *p35S::Luc* were
505 created using floral dipping in the *Col-0* background. *slr-1*×*pDR5::Luc* was generated
506 by crossing *slr-1* with *pDR5::Luc*.

507 **Plasmid construction and plant transformation**

508 To construct the *p35S::Luc* control plasmids, the *CaMV35S* promoter was inserted
509 upstream of the *Luciferase* gene in the pPLV03 vector[37]. Genomic DNA from
510 Arabidopsis ecotype Col-0 was used as the template for amplification of the upstream
511 promoter of AT4G14550 (IAA14) using the primers forward 5'-
512 ACAACTTTGTATAGAAAAGTTGTATGCCTCTCCACTACCACT -3' and reverse

513 5'- ACTGCTTTTTTGTACAAACTTGCTCTTCTTGCTGTCTATATATGT -3' and the
514 PCR product cloned into the pDONR P4-P1 vector (Invitrogen) and subsequently
515 recombined with the pENTR/D-TOPO-Luciferase clone[2] into the dpGreen-BarT
516 destination vector[38]. All constructs were verified by sequencing and introduced into
517 *Agrobacterium tumefaciens* strain GV3103 by electro-transformation, and
518 subsequently transformed into the *Col-0* ecotype background by floral dipping. The
519 harvested seeds were sown on soil and sprayed 0.2g/L Basta herbicide solution (Bayer)
520 for selecting positive *p35S::Luc* or *pIAA14::Luc* seedlings.

521 **Growth conditions and treatments**

522 The Arabidopsis seeds were sterilized for 2–5 minutes with 70% ethanol, followed by
523 drying. After sterilization, the seeds were uniformly plated on one single line on square
524 plates (12 × 12 × 1.5 cm). The plates contained 50 mL standard Murashige and Skoog
525 solid medium, which is made of 0.8% agar (Duchefa), 0.5× Murashige and Skoog (MS)
526 medium (Duchefa), and with 1% sucrose (MS+, no exogenous sucrose was added for
527 MS-) (pH 5.9). Subsequently, the seeds were stratified for 2 days in 10 °C and dark
528 conditions. Seeds were germinated on vertically positioned plates within a Weiss-
529 Technik incubator (Fitotron SGC 2), exposed to top-providing illumination from LED
530 white cultivation lights (16h day/8h night cycle) in 21 ºC and an irradiance of 120 μmol
531 m^{-2} s^{-1}. Plates grow under the above control condition for 4 days (root quantification
532 assay) or 5 days (luminescence monitoring assay) before subsequent experiments. For
533 light conditions and HT treatment, two Weiss-Technik incubators were configured at

534 either 21°C (control) or 29°C (HT), operating under constant light. Each incubator was
535 outfitted with top LED white culture lights arranged across three distinct culture levels,
536 featuring irradiances of 20, 50, and 120 (control) μmol m^{-2} s^{-1}.

537 **Root quantification**

538 For root phenotyping, surface-sterilized seeds were uniformly plated, stratified, and
539 germinated on a square plate (12 × 12 × 1.5 cm) as described above. After germination
540 under the control condition for 4 days, marking the position of the root tip, the 4-day-
541 old seedlings were then transferred to the treatment condition (either 21°C or 29°C with
542 light conditions set at 20, 50 or 120 μmol m^{-2} s^{-1}) for additional 3 days and the root tip
543 positions were marked again. For IAA and Auxinole treatment, water solution
544 containing 0.2 μM IAA (OlChemIm s.r.o.) or 20 μM Auxinole (OlChemIm s.r.o.) was
545 evenly spread on the plates, with solvent (DMSO, Duchefa) used as a control. For
546 lateral and primary root phenotyping, the plates were scanned at 600 dpi using an Epson
547 V850Pro photonegative scanner at 24-hour intervals, starting from the 3rd day to the
548 10th day of transferring. The lateral roots between the two marked root section were
549 counted manually from the images and the length of primary roots between two marked
550 positions was measured automatically using the SNT plugin or manually with
551 Fiji/ImageJ. The significance test was conducted in R using the t.test and aov functions.

552 **Lateral root primordia quantification**

553 To phenotype lateral root primordia, seeds were placed on individual square plates.
554 After marking the root tips of 4-day-old seedlings, they were moved to specific

555 treatment conditions as outlined in the manuscript and figure legend (either 21°C or
556 29°C with light conditions set at 50 or 120 μmol m^{-2} s^{-1}). Following a 3-day treatment,
557 the positions of the root tips were marked again, and the plates were scanned to measure
558 the length of the primary roots. After 5 days of treatment, primary roots located between
559 two marked positions were harvested, followed by fixation and clearing in accordance
560 with a previously published protocol[39]. The roots were mounted in 50% glycerol and
561 analyzed using a Zeiss AxioObserver Z1 microscope (Plan-Apochromat 40×/0.95
562 objective) with a AxioCam MRc camera. Primordia were counted manually, and the
563 length of primary roots between two marked positions was determined as described
564 above. The significance test was conducted in R using the aov functions.

565 **Luminescence imaging and analysis**

566 The luciferase activity in roots was visualized by time-lapse imaging of seedlings
567 sprayed with 2 mM luciferin (Biosynth AG, Switzerland). *DR5::Luciferase* seedlings
568 were grown using the general procedure as described above. To perform time-lapse
569 imaging of the *DR5:Luciferase* expression in the oscillation zone, a Vers Array XP
570 camera system (Roper Scientific) was used to image the luciferase signal in the vertical
571 growing Arabidopsis root tip from 5 days old (4 to 8 seedlings) with the set-up of the
572 exposure times of 5 min (binning 2) interrupted by 14 min LED WL (measured
573 irradiances of 10~30 μmol·m^{-2}·s^{-1} for low light, 40~60 μmol·m^{-2}·s^{-1} for medium light
574 and 110~130 μmol·m^{-2}·s^{-1} for high light condition) followed by 1 min darkness. The
575 temperature in the imaging chamber was configured at either 21°C or 29°C by a

576 recirculating Cooler (JULABO FL300). Image sequences were saved for further
577 analysis in Fiji/ImageJ. Image sequences were converted into kymographs by tracking
578 the final course of root growth. This visualization captures spatiotemporal changes in
579 Luciferase signals during primary root growth. To quantify the universal *DR5* signal in
580 primary roots, the grey value of the primary root excluding the tip to the oscillation
581 zone was recorded from the kymograph at an interval of every 10 hours. The PBS were
582 counted manually from the kymographs and original image sequences. The length of
583 primary roots was measured manually from the original images. To determine the time
584 and strength of the systemic *DR5* signal in primary roots, the time point and grey value
585 were recorded when the systemic *DR5* signal in the primary roots reached the top value.
586 To imaging luminescence of *p35S::Luc* control lines, seedlings were grown to 5-days-
587 old on solid MS+ medium sprayed with 2 mM luciferin (Biosynth AG, Switzerland)
588 following the general procedure as described above. Seedlings were then transferred
589 into Weiss-Technik incubators set to either 21°C (control) or 29°C (HT), with constant
590 illumination of 120 $\mu mol \cdot m^{-2} \cdot s^{-1}$ as described above. The images of luminescence in
591 primary root were captured using a FUSION SL4 system (VILBER), with 30 second
592 exposure at corresponding time points. The gray value of the primary root, excluding
593 the tip up to the oscillation zone (10 mm from root tip), was measured to assess the
594 universal luminescence signal in primary roots. All measurements were performed
595 manually with Fiji/ImageJ. The significance test was conducted in R using the t.test and
596 aov functions. The Anderson-Darling normality test was conducted in R using the
597 ad.test function.

598 **Supplementary References**

599 31. Reed J. W., et al., Phytochrome A and Phytochrome B Have Overlapping but
600 Distinct Functions in Arabidopsis Development. *Plant Physiol.* **104**, 1139-1149 (1994).
601 32. Reed J. W., et al., Mutations in the gene for the red/far-red light receptor
602 phytochrome B alter cell elongation and physiological responses throughout
603 Arabidopsis development. *Plant Cell* **5**, 147-157 (1993).
604 33. Guo H., et al., Regulation of Flowering Time by Arabidopsis Photoreceptors.
605 *Science* **279**, 1360-1363 (1998).
606 34. Leivar P., et al., Multiple phytochrome-interacting bHLH transcription factors
607 repress premature seedling photomorphogenesis in darkness. *Curr. Biol.* **18**, 1815-1823
608 (2008).
609 35. Oyama T., Shimura Y., Okada K., The Arabidopsis HY5 gene encodes a bZIP
610 protein that regulates stimulus-induced development of root and hypocotyl. *Genes Dev.*
611 **11**, 2983-2995 (1997).
612 36. Mazzella M. A., Casal J. J., Interactive signalling by phytochromes and
613 cryptochromes generates de-etiolation homeostasis in Arabidopsis thaliana. *Plant Cell*
614 *Environ.* **24**, 155-161 (2001).
615 37. De Rybel B., et al., A Versatile Set of Ligation-Independent Cloning Vectors for
616 Functional Studies in Plants. *Plant Physiol*. **156**, 1292-1299 (2011).
617 38. Lee JY., et al., Transcriptional and posttranscriptional regulation of transcription
618 factor expression in Arabidopsis roots. *Proc. Natl. Acad. Sci. U. S. A.* **103**, 6055–6060
619 (2006).

39. Malamy J. E., Benfey P. N., Organization and cell differentiation in lateral roots of Arabidopsis thaliana. *Development* **124**, 33-44 (1997).

Acknowledgements: We thank Stefan Kircher and Andreas Hiltbrunner for providing seed materials and critically reviewing the manuscript; Stefan Kircher for assistance with root luminescence imaging and analysis; Deutsche Forschungsgemeinschaft (DFG) (DFG; 470007283 to J.K.-V. and CIBSS – EXC-2189; 390939984 to J.K.-V.), Chinese Scholarship Council (CSC, 202006300036 to C.R.) and MICIU/AEI/10.13039/501100011033 (CEX2020-000999-S to M.A.M.-R. through CBGP) for funding.

Author contributions: C.R. and J.K.-V. designed the research; C.R. and J.B. performed the research; C.R. analyzed data; C. R. generated the *p35S::Luc* plasmid and plant material and M.A.M.-R. generated the *pIAA14:Luc* and *slr-1 × pDR5::Luc* plasmids and plant material; and C.R. and J.K.-V. wrote the paper. All authors edited the paper.

Competing interests: The authors declare no competing interests.

Additional Information: Correspondence and requests for materials should be addressed to J.K.-V (juergen.kleine-vehn@biologie.uni-freiburg.de).

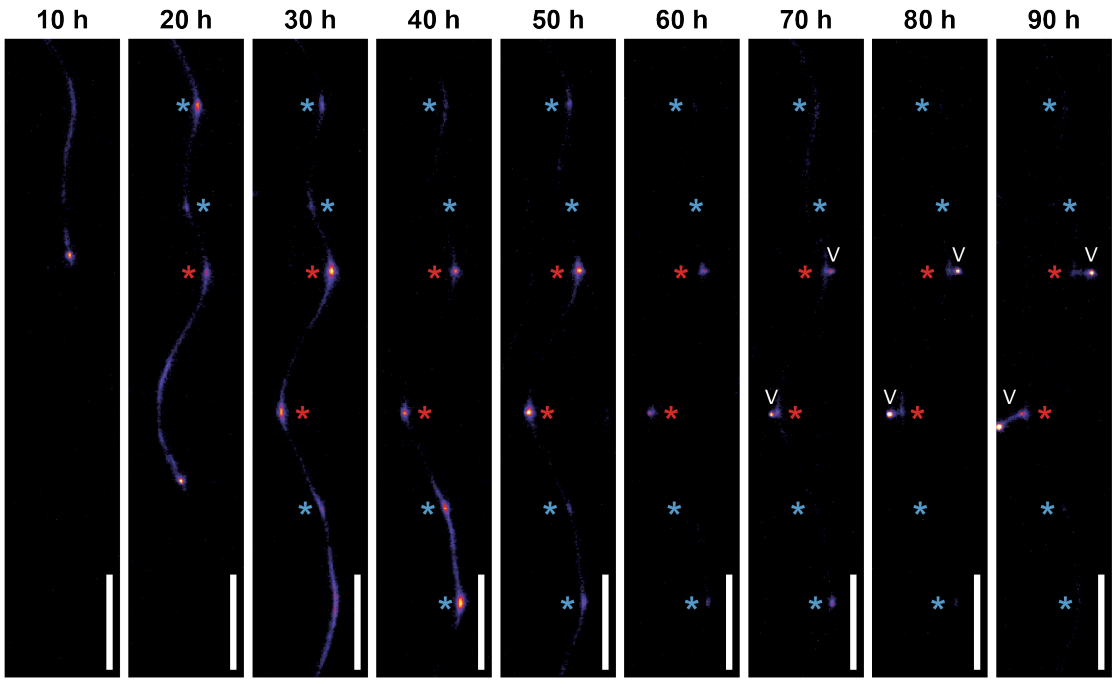

HL

Supplementary Figure 1. Original images showing the distinct progression of persistent and transient PBS at HL condition.

Time series images of the primary root were taken every 10 hours under 21°C and high light (HL) conditions. Persistent PBS is marked by a red asterisk and transient PBS is marked by a blue asterisk. The white arrowhead denotes the emerged lateral root (Scale bar = 1 mm).

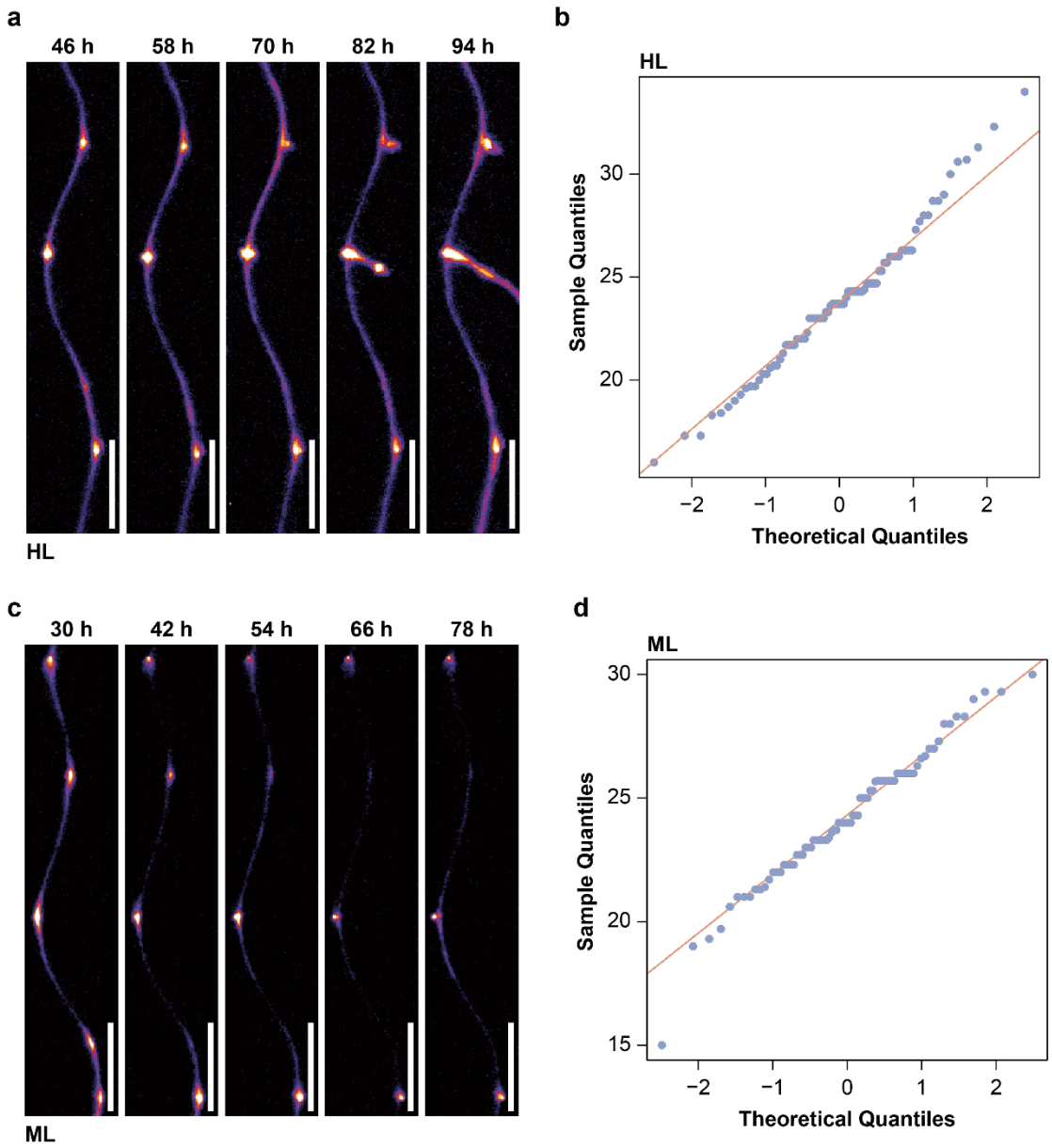

Supplementary Figure 2. The time intervals between oscillatory peaks of systemic auxin follow a normal distribution.

a, **c**, Time series images of the primary root were taken every 12 hours under high light (HL) (**a**) and medium light (ML) (**c**) at 21°C conditions (Scale bar = 1 mm). **b**, **d**, The quantile-quantile (Q-Q) plot compares the sample quantiles of the time intervals between peaks of systemic auxin oscillations with the corresponding theoretical

651 quantiles of normal distribution at 21°C and light intensities of HL (**b**) and ML (**d**)

652 conditions (n = 23 to 29). The pattern closely following the orange line indicates that

653 the frequency of the systemic oscillation is likely to follow a normal distribution.

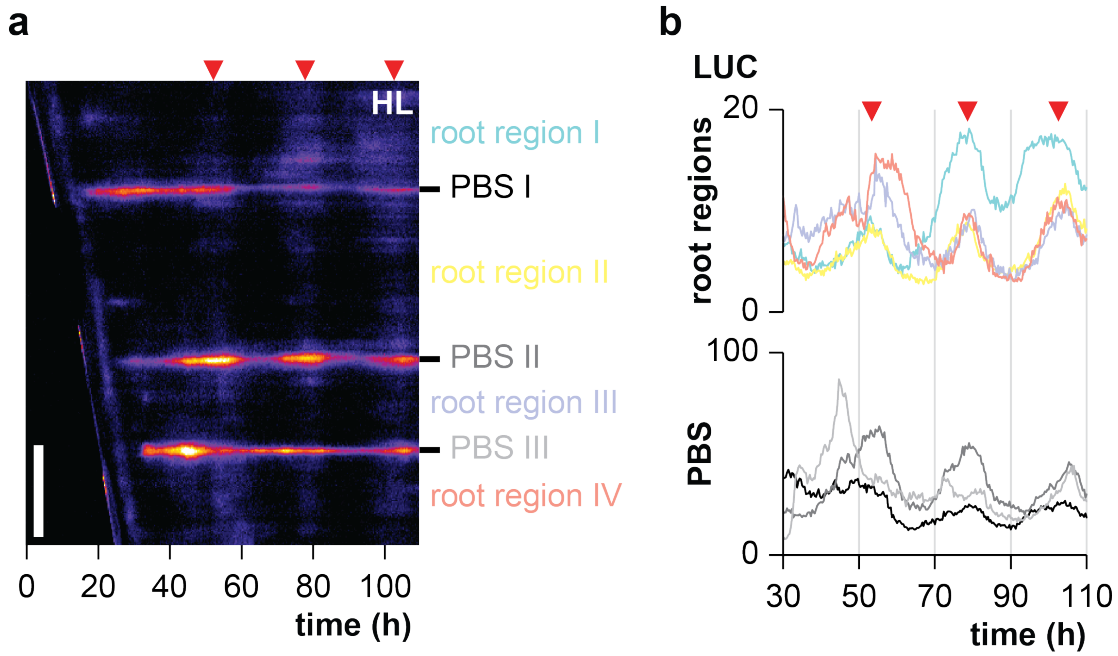

654

655 **Supplementary Figure 3. Kymograph showing the distinct progression of**

656 **persistent and transient PBS at HL condition.**

657 **a**, **b**, Kymograph (**a**) and real-time quantification (**b**) of luminescence display auxin

658 signalling dynamics in specific root regions and PBS, with red triangles mark

659 oscillatory peaks of systemic auxin signal (Scale bar = 1 mm). The colored notation on

660 the right of (**a**) marks the quantified root regions and PBS, corresponding to the same

661 colors in (**b**).

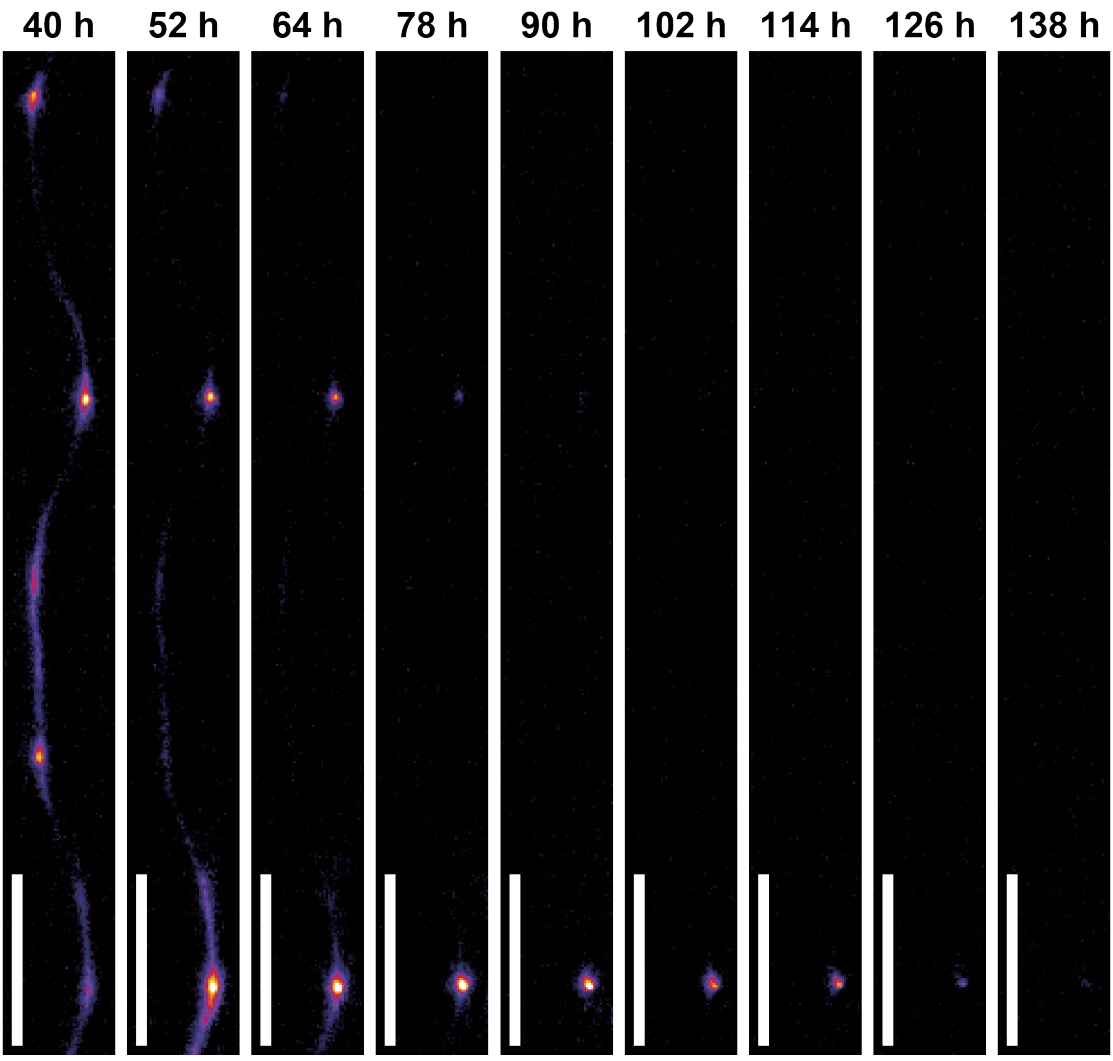

Supplementary Figure 4. Original images showing the dynamic of systemic auxin signal and progression of PBS at low light conditions.

Time series images of the primary root were taken every 12 hours under 21°C and low light (LL) conditions (Scale bar = 1 mm).

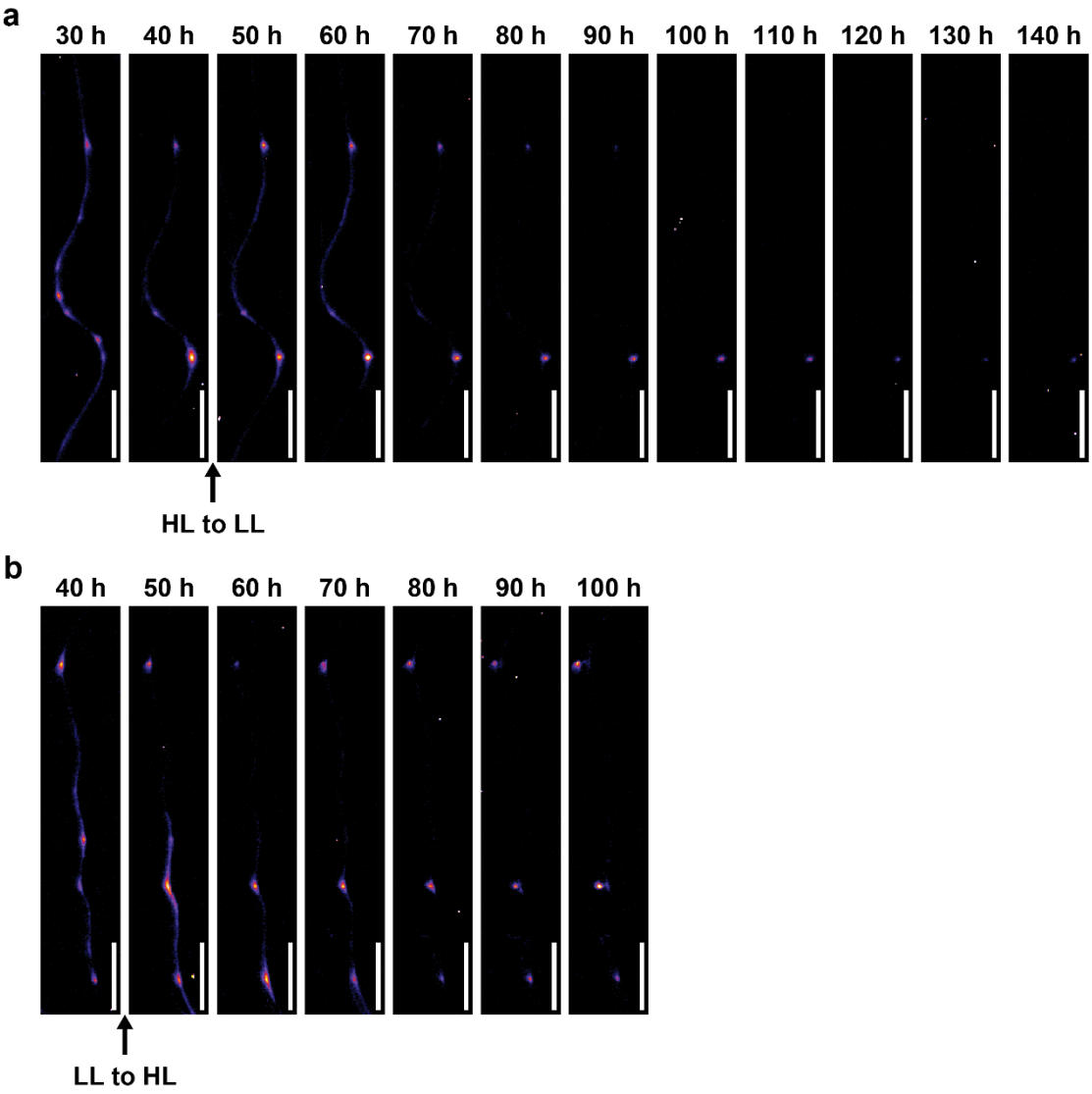

Supplementary Figure 5. Original images showing the dynamic of systemic auxin signal and progression of PBS during light transitions.

a, **b**, Time series images of the primary root were taken every 12 hours under light transitional conditions from high light (HL) to low light (LL) (**a**), and from LL-to-HL (**b**) (Scale bar = 1 mm).

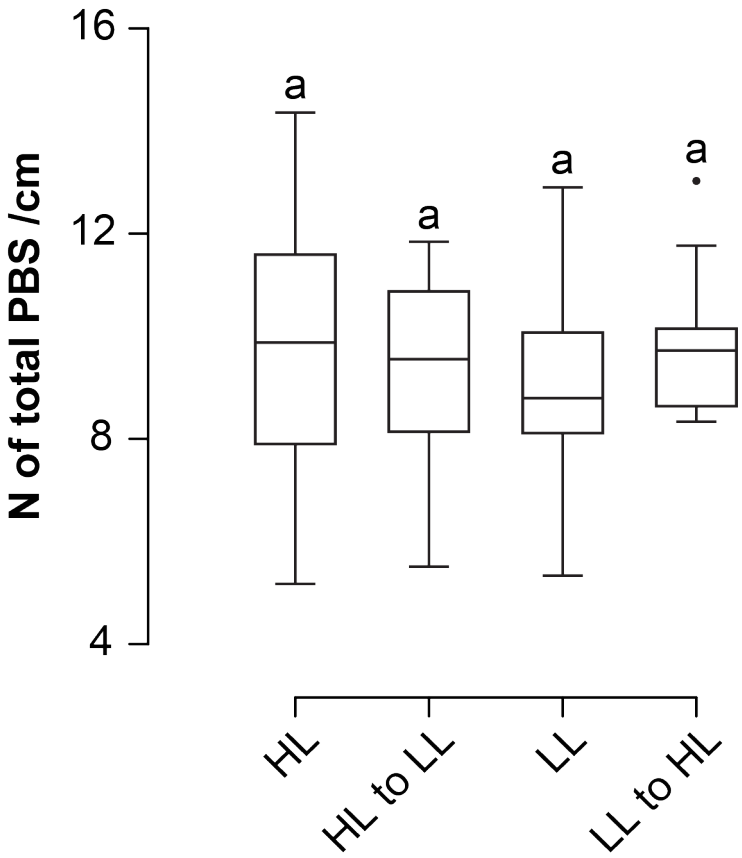

Supplementary Figure 6. The density of total PBS is quantitatively comparable at maintained and fluctuating light conditions.

Quantification of total PBS density under high light (HL), low light (LL) and transfer from HL-to-LL and LL-to-HL conditions (n = 16 to 38). Letters indicate values with statistically significant differences from one-way ANOVA performed ($P > 0.05$).

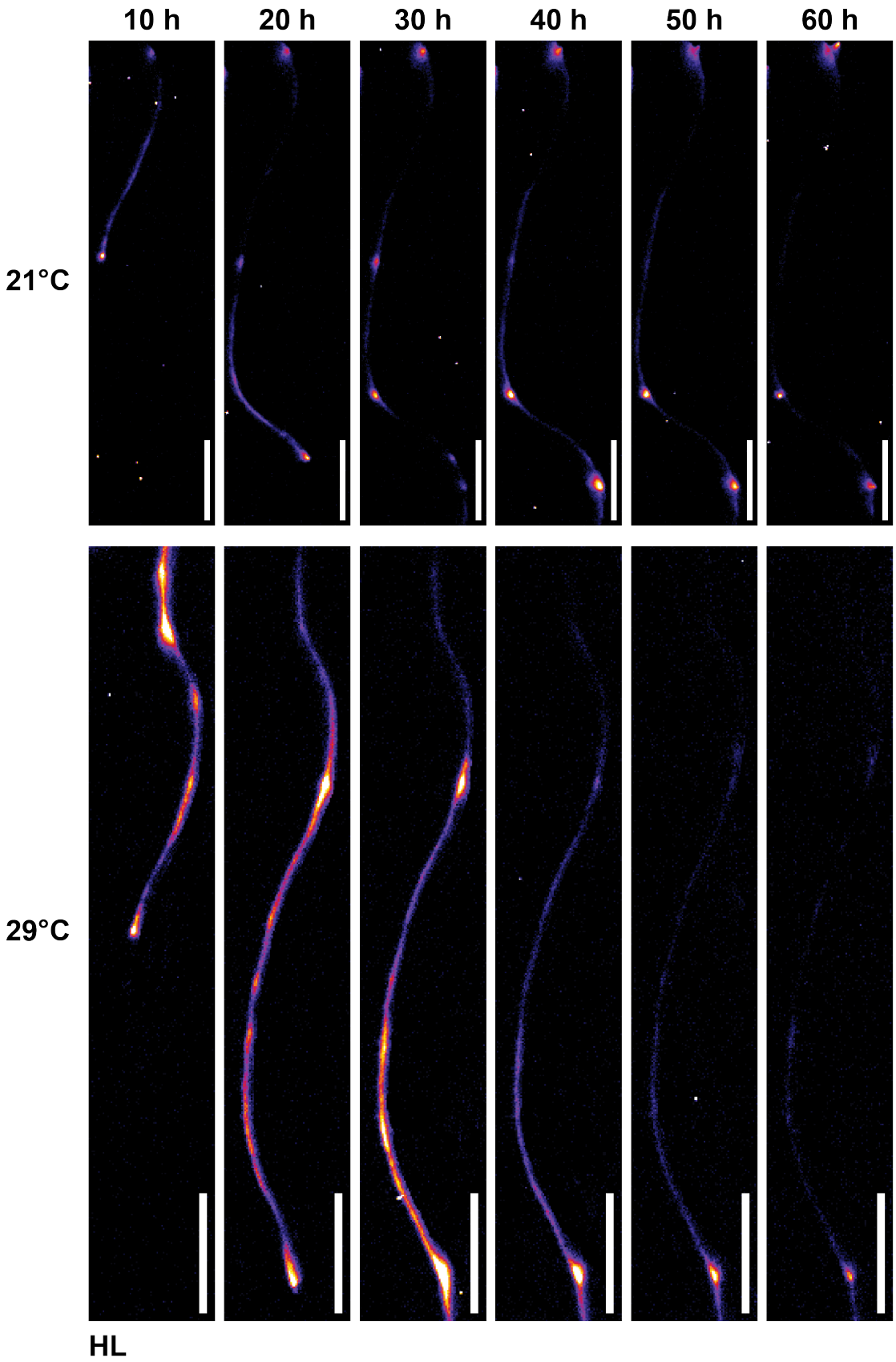

679

680 **Supplementary Figure 7. Original images showing the dynamic of systemic auxin**

signal and progression of PBS under 21°C and 29°C at high light conditions.

Time series images of the primary root were captured every 10 hours under high light (HL) conditions at 21°C (top row) and 29°C (bottom row) (Scale bar = 1 mm).

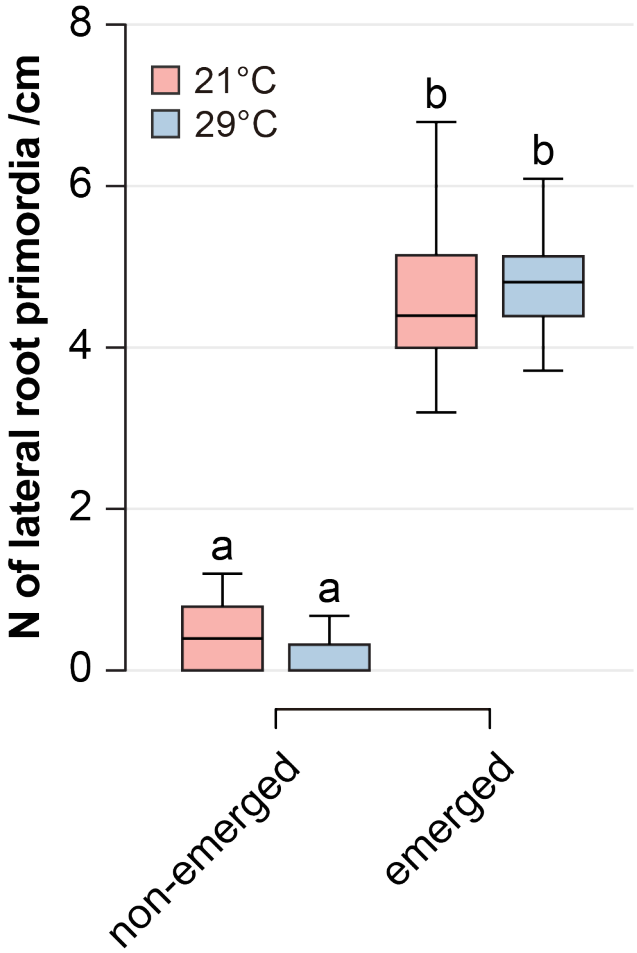

Supplementary Figure 8. Density of lateral root primordia is quantitively comparable between 21°C and 29°C at high light conditions.

Quantification of lateral root primordia density at 21°C and 29°C under high light conditions (n = 34 to 38). Letters indicate values with statistically significant differences from one-way ANOVA performed ($P < 0.0001$).

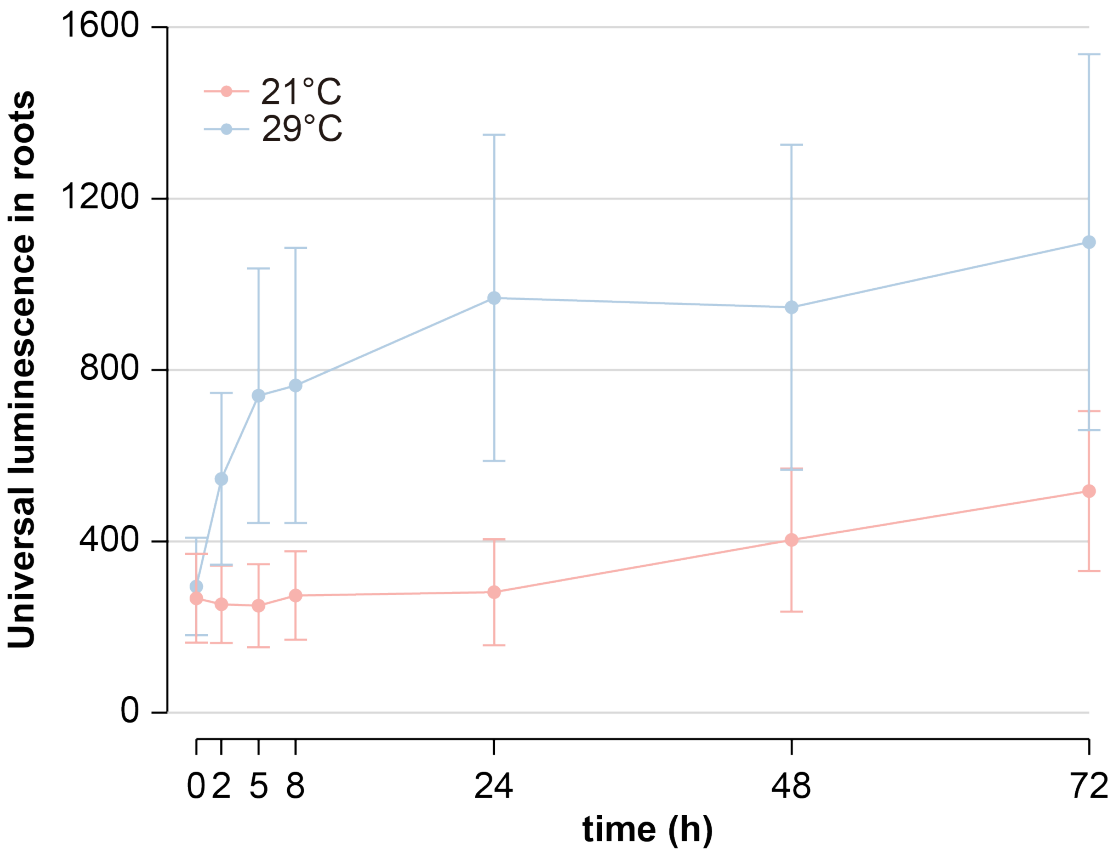

690

691 **Supplementary Figure 9. Time series quantification of universal *p35S::Luc* signal**

692 **in primary roots at 21°C and 29°C.**

693 Quantification of luminescence in primary roots showing the dynamics of the

694 *p35S::Luc* signal at 21°C and 29°C under high light conditions (Error bars represent

695 standard deviation; n = 45 to 47).

696

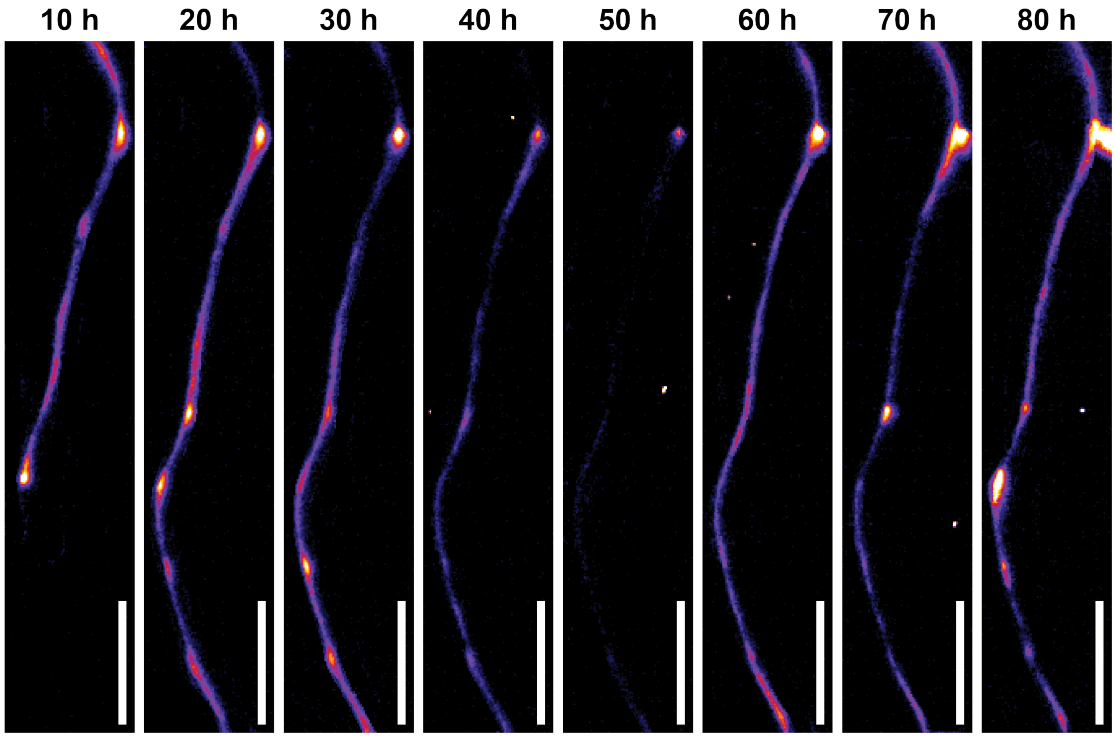

HL

Supplementary Figure 10. Original images showing the recovery of systemic auxin signal and PBS under high temperature at high light conditions.

Time series images of the primary root were captured every 10 hours under high light (HL) conditions at 29°C. Scale bar = 1 mm.

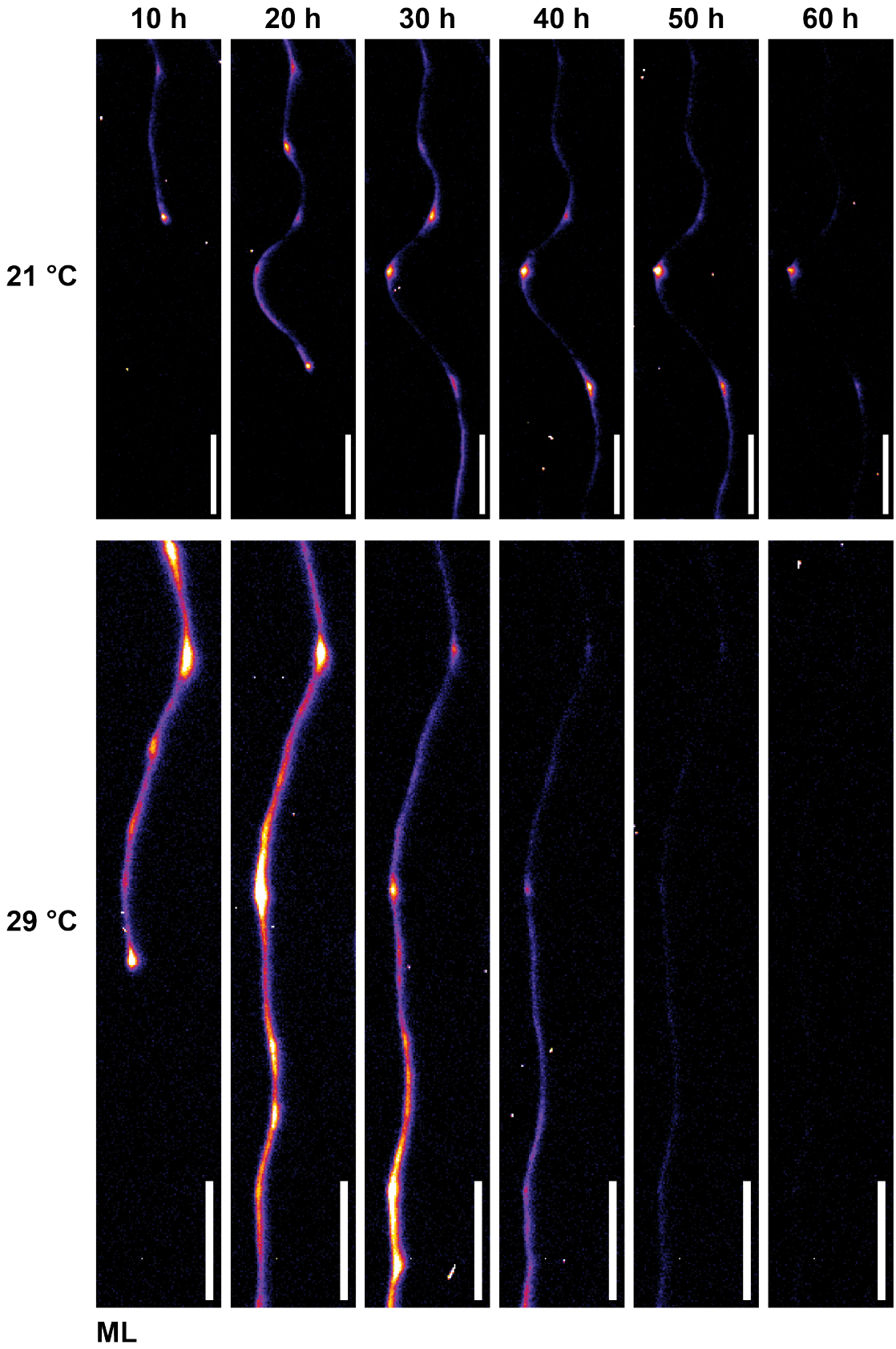

Supplementary Figure 11. Original images showing the dynamic of systemic auxin

704 **signal and progression of PBS under 21°C and 29°C at medium light conditions.**

705 Time series images of the primary root were captured every 10 hours at 21°C (top row)

706 and 29°C (bottom row) under medium light (ML) conditions (Scale bar = 1 mm).

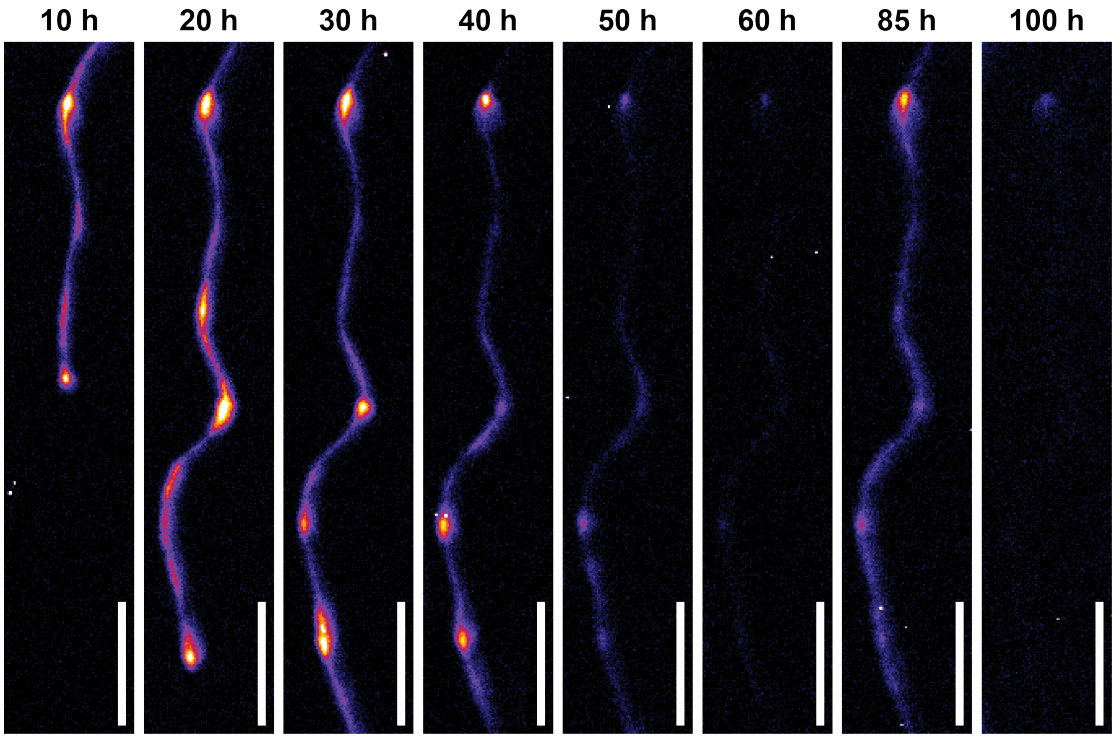

707 **ML & 29°C**

708 **Supplementary Figure 12. Original images showing the recovery of systemic auxin**

709 **signal and PBS under high temperature at medium light conditions.**

710 Time series images of the primary root were captured every 10 hours under 29°C and

711 medium light (ML) conditions (Scale bar = 1 mm).

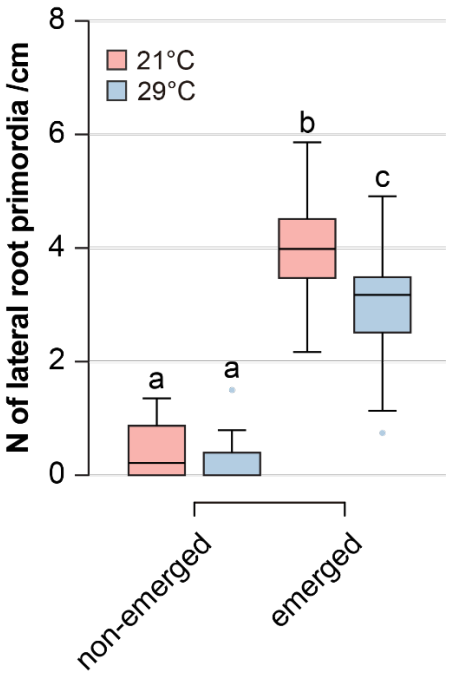

Supplementary Figure 13. Density of lateral root primordia under 21°C and 29°C at medium light conditions.

Quantification of lateral root primordia density at 21°C and 29°C under medium light conditions (n = 32 to 34). Letters indicate values with statistically significant differences from one-way ANOVA performed ($P < 0.0001$).

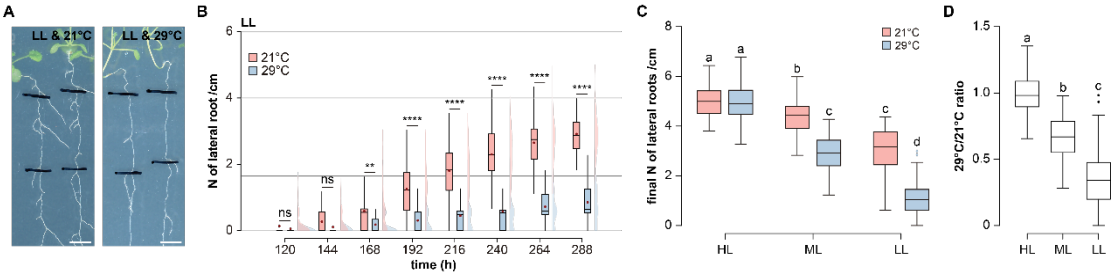

Supplementary Figure 14. Light quantity modulates the high temperature-dependent inhibition of lateral root density.

a, **b**, Representative images of root systems (**a**) and time series quantification of LR

density (**b**) at 21°C and 29°C under low light (LL) conditions (*n* = 53 to 55; Scale bar = 5 mm). **c**, **d**, Quantification (**c**) and calculated ratio (**d**) of final LR density at 21°C and 29°C under high light (HL), medium light (ML) and LL conditions (*n* = 53 to 55). Letters indicate values with statistically significant differences from one-way ANOVA performed for (**c**) and (**d**) ($P < 0.0001$ for both).

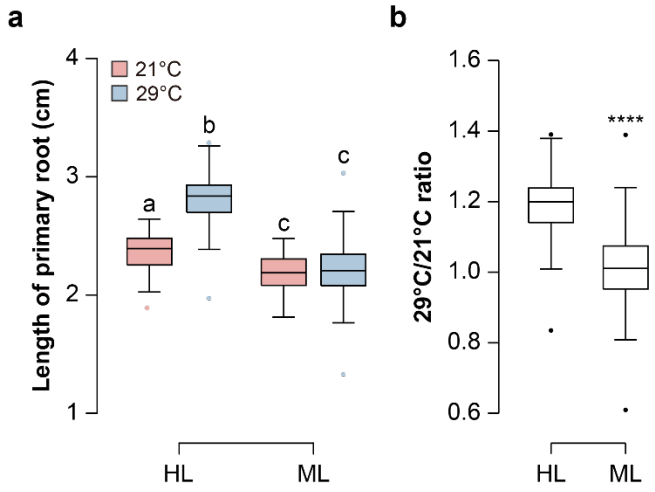

Supplementary Figure 15. High temperature-dependent elongation of the primary root relies on light.

a, **b**, Quantification (**a**) and Calculated ratio (**b**) of primary root length of *Col-0* at 21°C and 29°C under high light (HL) and medium light (ML) (*n* = 54 to 55). Letters indicate values with statistically significant differences from one-way ANOVA performed for (**a**) ($P < 0.0001$). Paired and two-tailed student's t-test performed for (**b**) ($P < 0.0001$****).

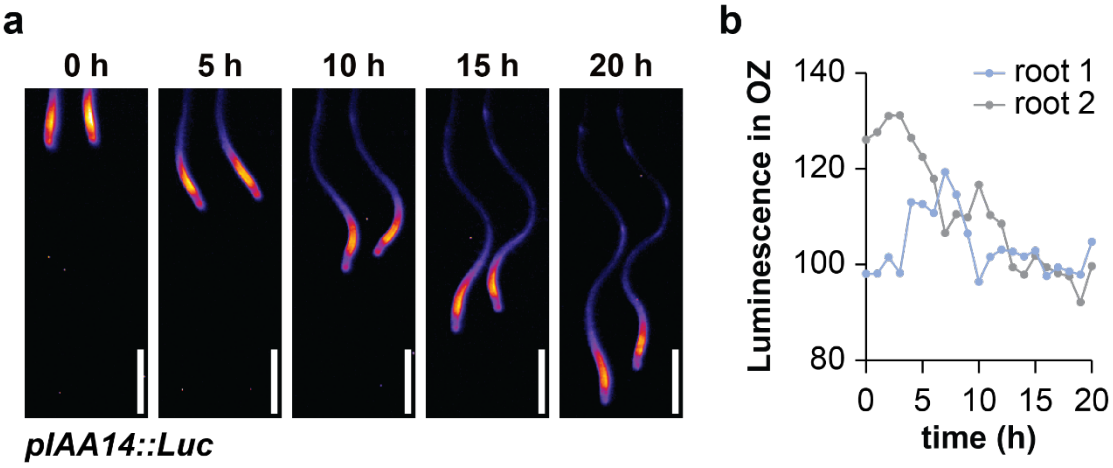

Supplementary Figure 16. Original images and quantification showing the dynamic of *IAA14* reporter in oscillation zone.

a, Time series images of the primary root were captured every 5 hours under 21°C and HL conditions (Scale bar = 1 mm). **b**, Time series luminescence quantification in the oscillation zone (OZ) of two independent roots.

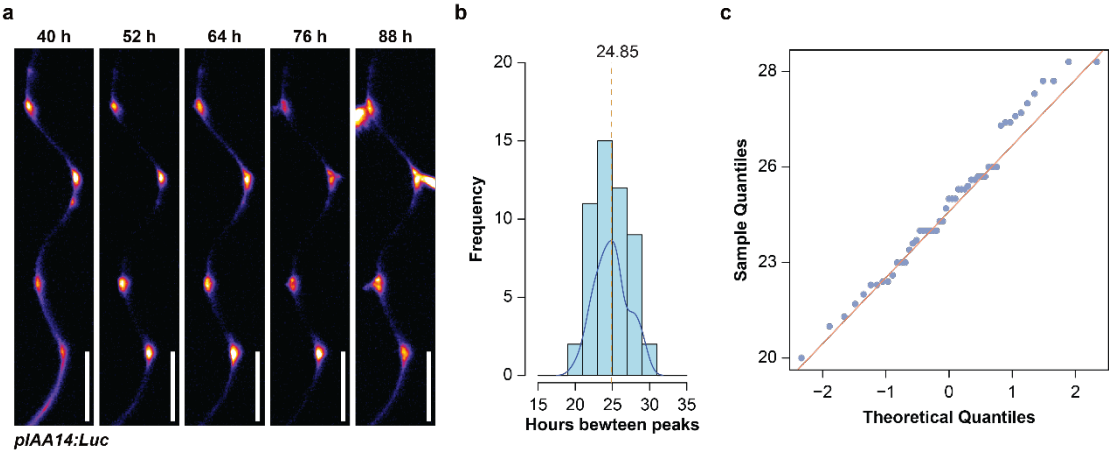

Supplementary Figure 17. The time intervals between oscillatory peaks of *IAA14* reporter signal follows a normal distribution.

a, Time series images of the *pIAA14::Luc* primary root were taken every 12 hours under

745 high light (HL) at 21°C conditions (Scale bar = 1 mm). **b**, Quantified distribution of the
746 time intervals between oscillatory peaks of *IAA14* reporter signal under high light (HL)
747 at 21°C conditions (mean value marked by a yellow dashed line; n = 17). **c**, The
748 quantile-quantile (Q-Q) plot compares the sample quantiles of the time intervals
749 between peaks of *IAA14* reporter oscillations with the corresponding theoretical
750 quantiles of normal distribution at 21°C and light intensities of HL (n = 17). The pattern
751 closely following the orange line indicates that the frequency of the systemic oscillation
752 is likely to follow a normal distribution (Anderson-Darling normality test, P-value =
753 0.4336).

754 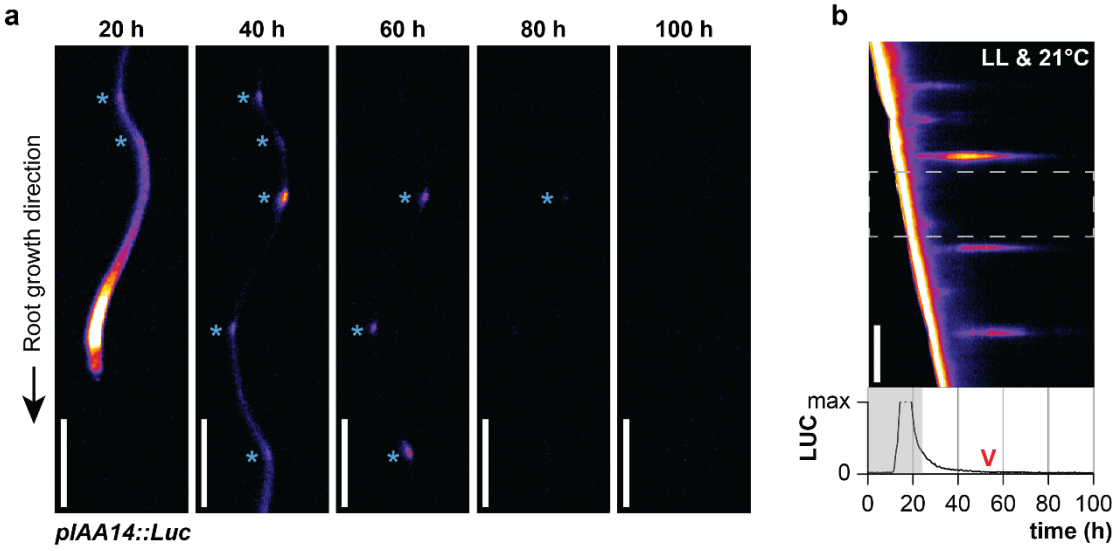

755 **Supplementary Fig. 18. Original images and kymograph showing the dynamic of**
756 ***IAA14* reporter signal and progression of PBS at low light conditions.**

757 **a**, Time series images of the *pIAA14::Luc* primary root under low light (LL) at 21°C
758 conditions (Scale bar = 1 mm). Blue asterisks mark transient PBS. **b**, Kymograph
759 showing dynamic of *pIAA14::Luc* and progression of PBS under LL at 21°C conditions

760 (Scale bar = 1 mm). Quantification of real-time luminescence is below the kymographs
761 where the red arrowhead denotes the downregulation of the *pIAA14::Luc* signal. The
762 dashed grey rectangle in the kymographs mark the region for the real-time plots. The
763 shaded area in real-time plots marks the signal originating from the root tip and local
764 oscillation (root clock) zone.

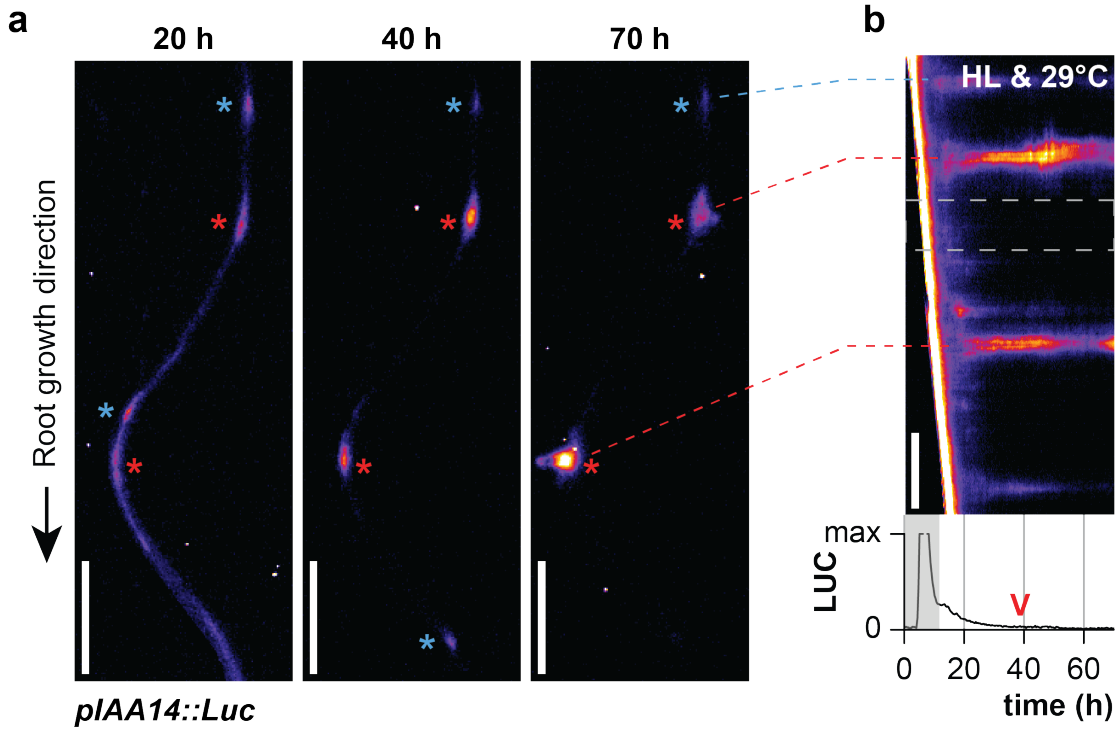

765

766 **Supplementary Fig. 19. Original images and kymograph showing the dynamic of**
767 ***IAA14* reporter signal and PBS under high temperature and high light conditions**.

768 **a**, Time series images of the *pIAA14::Luc* primary root under high light (HL) at 29°C
769 conditions (Scale bar = 1 mm). Red asterisks mark persistent PBS and blue asterisks
770 mark transient PBS. **b**, Kymograph showing dynamic of *pIAA14::Luc* and progression
771 of PBS under HL at 29°C conditions (Scale bar = 1 mm). Quantification of real-time
772 luminescence is below the kymographs where the red arrowhead denotes the

773 downregulation of the *pIAA14::Luc* signal. The dashed grey rectangle in the
774 kymographs mark the region for the real-time plots. The shaded area in real-time plots
775 marks the signal originating from the root tip and local oscillation (root clock) zone.

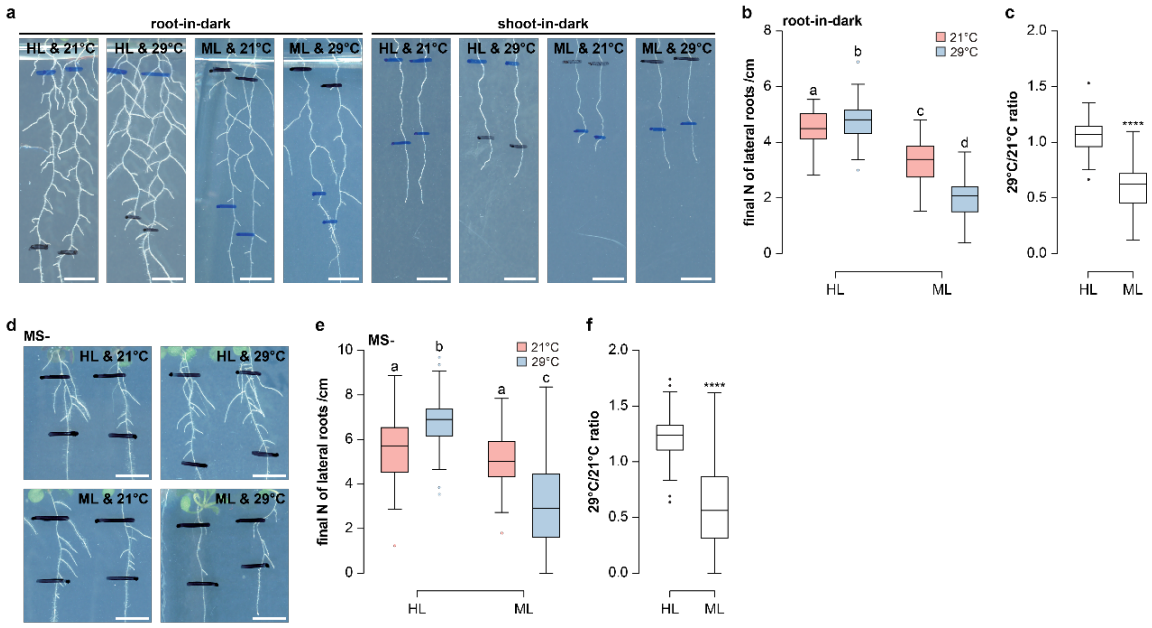

776

777 **Supplementary Figure 20. Shoot-received light modulates the high temperature-**
778 **dependent inhibition of lateral root density while sucrose is mechanically distinct.**

779 **a**, Representative images of root systems at 21°C and 29°C under root-in-dark and
780 shoot-in-dark conditions(Scale bar = 5 mm). **b**, **c**, Quantification (**b**) and calculated
781 ratio (**c**) of LR density at 21°C and 29°C under root-in-dark conditions (n = 50 to 61).
782 **d**, Representative images of root systems at 21°C and 29°C under high light (HL) and
783 medium light (ML) conditions on solid medium without sucrose (MS-) plates (Scale
784 bar = 5 mm). **e**, **f**, Quantification (**e**) and calculated ratio (**f**) of LR density of seedlings
785 grown at 21°C and 29°C under HL and ML conditions on MS- plates (n = 47-51). Paired
786 and two-tailed student's t-test performed for (**c**) and (**f**) (P < 0.0001**** for both).

Letters indicate values with statistically significant differences from one-way ANOVA performed for (**b**) and (**e**) ($P < 0.0001$ for both).

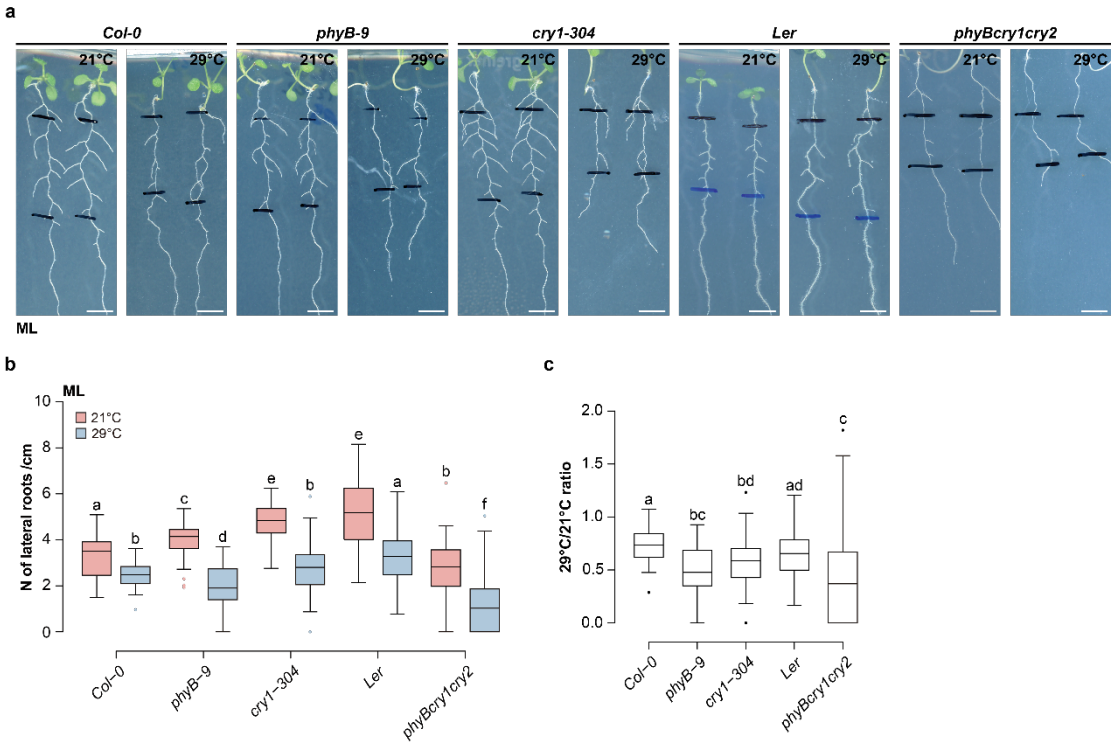

Supplementary Figure 21. The loss of PHYB and CRY1 enhances the HT-dependent inhibition of LR under ML conditions.

a-c, Representative root system images (**a**) and quantification (**b**) as well as the calculated ratio (**c**) of LR density in *Col-0*, *phyB-9*, *cry1-304*, *Ler* and *phyBcry1cry2* at 21°C and 29°C under medium light (ML) conditions (n = 51 to 90; Scale bar = 5 mm). Letters indicate values with statistically significant differences from one-way ANOVA performed for (**b**) and (**c**) ($P < 0.0001$ for both).

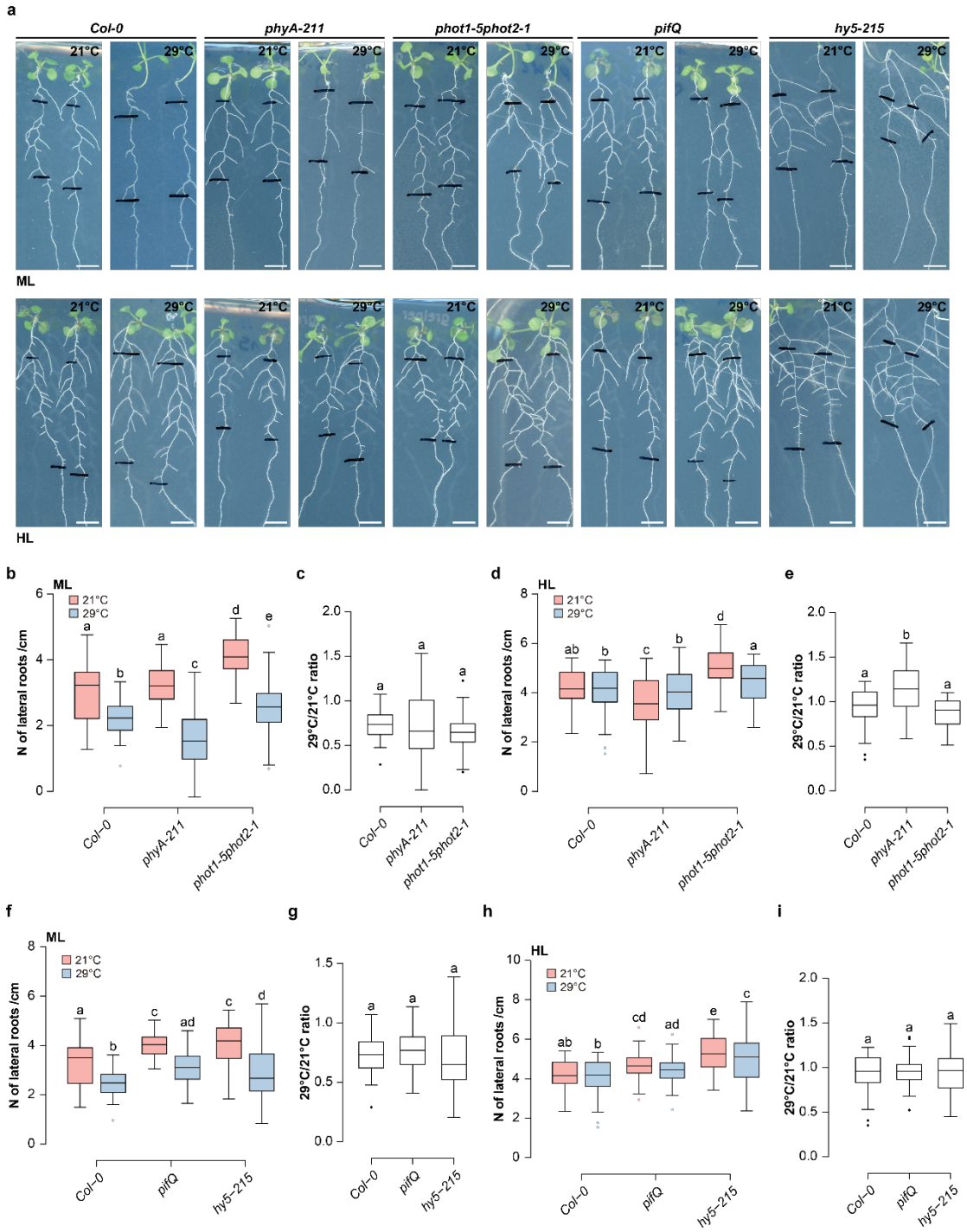

Supplementary Figure 22. The inhibition of lateral rooting under high-temperature conditions in light signalling mutants.

a, Representative root system images of wild-type *Col-0* and light signalling mutants at 21°C and 29°C under medium light (ML) (top row) and high light (HL) (bottom row)

802 conditions (Scale bar = 5 mm). **b**, **c**, Quantification (**b**) and calculated ratio (**c**) of LR
803 density in *Col-0*, *phyA-211* and *phot1-5phot2-1* at 21°C and 29°C under ML conditions
804 (n = 45 to 54). **d**, **e**, Quantification (**d**) and calculated ratio (**e**) of LR density in *Col-0*,
805 *phyA-211* and *phot1-5phot2-1* at 21°C and 29°C under HL conditions (n = 52 to 54). **f**,
806 **g**, Quantification (**f**) and calculated ratio (**g**) of LR density in *Col-0*, *pifQ* and *hy5-215*
807 at 21°C and 29°C under ML conditions (n = 52 to 54). **h**, **i**, Quantification (**h**) and
808 calculated ratio (**i**) of LR density in *Col-0*, *pifQ* and *hy5-215* at 21°C and 29°C under
809 HL conditions (n = 53 to 54). Letters indicate values with statistically significant
810 differences from one-way ANOVA performed for (**b**), (**d**), (**e**), (**f**) and (**h**) ($P < 0.0001$
811 for all) and for (**c**), (**g**) and (**i**) ($P > 0.05$ for all).